

Interactions between Large Molecules: Puzzle for Reference Quantum-Mechanical Methods

Yasmine S. Al-Hamdani[‡]

*Department of Chemistry, University of Zurich, CH-8057 Zürich, Switzerland and
Department of Physics and Materials Science,
University of Luxembourg, L-1511 Luxembourg, Luxembourg*

Péter R. Nagy[‡]

*Department of Physical Chemistry and Materials Science,
Budapest University of Technology and Economics,
H-1521 Budapest, P.O.Box 91, Hungary*

Dennis Barton

*Department of Physics and Materials Science,
University of Luxembourg, L-1511 Luxembourg, Luxembourg*

Mihály Kállay

*Department of Physical Chemistry and Materials Science,
Budapest University of Technology and Economics,
H-1521 Budapest, P.O.Box 91, Hungary*

Jan Gerit Brandenburg*

*Interdisciplinary Center for Scientific Computing, University of Heidelberg,
Im Neuenheimer Feld 205A, 69120 Heidelberg, Germany and
Digital Organization, Merck KGaA,
Frankfurter Str. 250, 64293 Darmstadt, Germany*

Alexandre Tkatchenko[‡]

*Department of Physics and Materials Science,
University of Luxembourg, L-1511 Luxembourg, Luxembourg*

[‡]These authors contributed equally.

Abstract

Quantum-mechanical methods are widely used for understanding molecular interactions throughout biology, chemistry, and materials science. Quantum diffusion Monte Carlo (DMC) and coupled cluster with single, double, and perturbative triple excitations [CCSD(T)] are two state-of-the-art and trusted wavefunction methods that have been categorically shown to yield accurate interaction energies for small organic molecules. These methods provide valuable reference information for widely-used semi-empirical and machine learning potentials, especially where experimental information is scarce. However, agreement for systems beyond small molecules is a crucial remaining milestone for cementing the benchmark accuracy of these methods. Approaching such well-converged predictive power in larger molecules has motivated major developments in CCSD(T) as well as DMC algorithms in the past years, resulting in orders of magnitude time-to-solution reductions. Here, we show that CCSD(T) and DMC interaction energies are not in consistent agreement for a set of polarizable supramolecules. Whilst agreement is found for some of the complexes, in a few key systems disagreements of up to 8 kcal mol⁻¹ remained. This leads to differences of up to 6 orders of magnitude in the corresponding binding association constant at room temperature for systems which are well within the accustomed domain of applicability for both methods. These findings thus indicate that more caution is required when aiming at reproducible non-covalent interactions between extended molecules. Our data contradicts the expectation that the most comprehensive and robust wavefunction methods predict identical non-covalent interactions and indicate an unsolved challenge for benchmark approaches.

* j.g.brandenburg@gmx.de

† alexandre.tkatchenko@uni.lu

MAIN

The most accurate methods for studying matter at the atomic scale are wavefunction-based approaches which explicitly account for many-electron interactions. Given only the positions and nuclear charges of atoms, we can now predict, among basically every observable property, the binding strength of relatively small molecular systems (*i.e.* less than 50 atoms) to within a few tenths of a kcal mol⁻¹ using many-body solutions to the Schrödinger equation [1–3]. This value is better than the so-called “chemical accuracy” of 1 kcal mol⁻¹ required for reliable predictions of thermodynamic properties. Indeed, the relative stabilities of many non-covalently bound materials such as 2D layered materials, pharmaceutical drugs, and different polymorphs of ice, are underpinned by small energy differences on the order of tenths of a kcal mol⁻¹ [4]. However, experimentally determining binding affinities under well-defined, pristine conditions is notoriously challenging [5]. In addition, thousands of computational works describe physical interactions in materials, which are not well understood at the experimental level, for instance, as part of rational design initiatives in novel materials including soft colloidal matter, nanostructures, metal organic and covalent organic frameworks [6–8]. The present shortage of benchmark information is a major setback for forming reliable predictions across the natural sciences and is frequently addressed through demanding, but increasingly feasible, wavefunction-based methods. However, extending the use of highly-accurate methods to a regime of larger molecules is hindered by theoretical and technical challenges due to the steep increase in computational cost required for an accurate description of many-electron interactions [9, 10].

Here we use two widely trusted wavefunction methods that can provide sub-chemically accurate solutions to the electronic Schrödinger equation for non-covalent interactions. First, we utilize coupled-cluster (CC) theory with single, double, and perturbative triple excitations [CCSD(T)] [12] – approximated via the local natural orbital (LNO) scheme to be practicable [LNO-CCSD(T)] [13, 14]. Coupled cluster theory has gained great prominence in the last 30 years and the label of ‘gold-standard’ for remarkable accuracy on virtually all systems in its domain of applicability [15]. Second, a stochastic quantum method that computes the energy for the many-electron wavefunction directly is known as fixed-node diffusion Monte Carlo (FN-DMC). This method has seen a surge of use in recent years, particularly for predicting large molecules and periodic systems with non-covalent interactions [10, 16], such

as molecular crystals and adsorption on 2D materials [16–18].

As we demonstrate in Fig. S1, CCSD(T) and FN-DMC interaction energies are in sub-chemical agreement in small systems such as the benzene-water dimer [11]. Nonetheless, FN-DMC and CCSD(T) are still prohibitively expensive for most applications in biology and chemistry, and as result, very little is known about how predictive these theoretical methods are in the regime of larger molecules.

Straightforward extrapolations of interactions from small molecules to large complexes are difficult to make due to the interplay and accumulation of interactions that are non-additive, anisotropic, or have many-body character [11, 19–22]. As such, a deeper understanding of non-covalent interactions can be gained by directly applying state-of-the-art methods in larger molecular complexes. Here, we use a frequently studied compilation, the L7 molecular data set from Sedlak *et al.* [23] to ascertain the predictive power of FN-DMC and CCSD(T) for relatively large complexes involving intricate $\pi - \pi$ stacking, electrostatic interactions, and hydrogen-bonding (see Fig. S2). In addition, we consider a larger system of a C₆₀ buckyball inside a [6]-cycloparaphenyleneacetylene ring (which we label as C₆₀@[6]CPPA), consisting of 132 atoms. This structure has a number of interesting features: (i) an open-

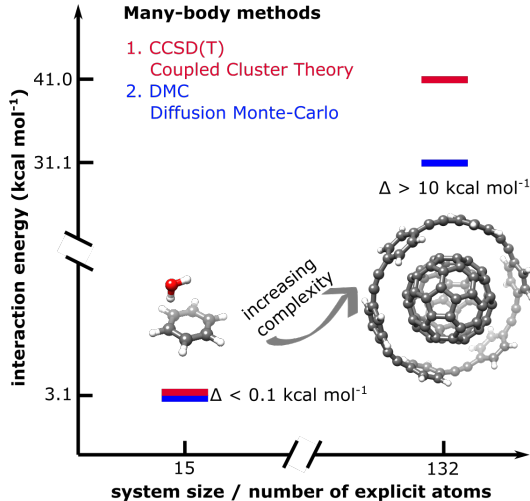


FIG. S1. The CCSD(T) and FN-DMC computed binding energies of a water-benzene dimer [11] is shown in comparison to a buckyball-ring complex computed here. It can be seen that the binding energy increases by a factor ~ 10 , near-linearly with the size of the system, whereas the corresponding disagreement between CCSD(T) and FN-DMC increases by a factor of ~ 100 .

framework that can be found in covalent organic frameworks and carbon nanotubes, (ii) the buckyball has a large polarizability ($76 \pm 8 \text{ \AA}^3$) [24] which gives rise to considerable dispersion interactions, and (iii) confinement between the ring and the buckyball that may cause non-trivial long-range repulsive interactions [25].

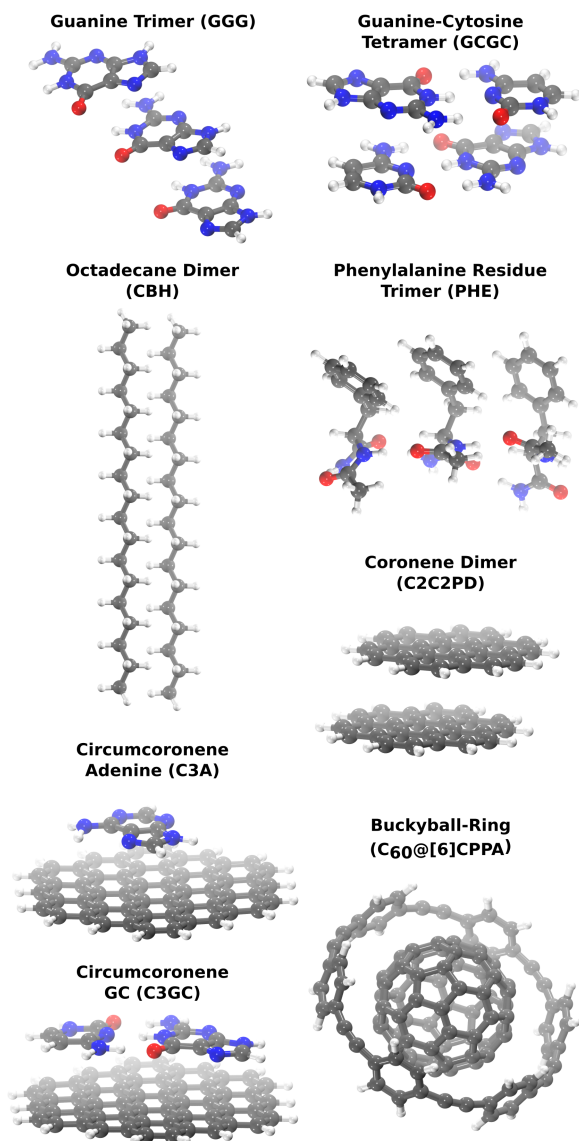


FIG. S2. The supramolecular complexes from L7 data set [23] and a buckyball-ring supramolecular complex consisting of 132 atoms.

Following recent algorithmic advances for more efficient CCSD(T) and FN-DMC, we predict interaction energies for a set of supramolecular complexes and converge numerical thresholds to the best of our joint knowledge and expertise. Hereafter, we refer to CCSD(T)

and FN-DMC interaction energies but note that a number of approximations are used in both methods. More specifically, the CCSD(T) interaction energies we report come from systematically converging LNO-CCSD(T) towards canonical CCSD(T). Meanwhile, the significance of approximations in FN-DMC interaction energies are assessed using statistical measures. CCSD(T) and FN-DMC are consistent for five of the eight supramolecular complexes, covering a range of interactions including hydrogen bonding and $\pi - \pi$ stacking. However, we find that three key complexes reveal several kcal mol⁻¹ differences between best estimated CCSD(T) and FN-DMC calculations. Most notably, a substantial disagreement of ~ 8 kcal mol⁻¹ (or 20 %) is found in the interaction energy (E_{int} as defined in Methods) of the buckyball-ring system. This 8 kcal mol⁻¹ inconsistency remains on top of the uncertainty estimates incorporating all controllable sources of errors. We also gauge the impact of approximations intrinsic to each method, not covered in the numerical uncertainty estimates, and find that 8 kcal mol⁻¹ is an order of magnitude beyond these. It is thus yet unclear whether this discrepancy would also be present between the approximation-free CCSD(T) and DMC results or it is a result of an unexplored source of error. As shown in Fig. S1 and in Table SI below, such a sizable deviation cannot be explained solely by the size-extensive growth of the difference between CCSD(T) and FN-DMC. Consequently, the interaction energies of three of the complexes considered here are still unsettled.

We applied two different, widely-used and well-performing DFT approaches developed for capturing long-range dispersion interactions: DFT+D4 [26] and DFT+MBD [27]. Both methods model London dispersion based on a coarse-grained description and account for all orders of many-body dispersion in different manner. See Refs. [28, 29] for an overview of various ways to capture dispersion in the DFT framework. We find that DFT+MBD closely matches FN-DMC, while the recent DFT+D4 method agrees well with CCSD(T), irrespective of the level of disagreement between CCSD(T) and FN-DMC. Therefore, the absence of either CCSD(T) or FN-DMC references could incorrectly suggest that one of the DFT methods performs better than the other. This illustrates that the unprecedented level of disagreement amongst state-of-the-art methods in large organic molecules has consequences well outside the developer communities.

State-of-the-art methods for non-covalent interactions

CCSD(T) and FN-DMC methods account for dynamic electron correlation through an expansion in electron configurations in the former and through the real-space fluctuation of electrons in the latter. These two equally viable formulations can be illustrated by the corresponding expressions of $\Psi(\mathbf{R})$, the exact wavefunction:

1. **DMC:** Imaginary time (τ) propagation of a trial function $\Psi_T(\mathbf{R})$ in real space:

$$|\Psi(\mathbf{R})\rangle = \lim_{\tau \rightarrow \infty} \exp\left[-\tau(\hat{H} - E_T)\right] |\Psi_T(\mathbf{R})\rangle$$

2. **CC:** Expansion of excited determinants generated via the operator \hat{T}_n from a reference wavefunction: $|\Psi(\mathbf{R})\rangle = \exp\left[\sum_{n=1}^{\infty} \hat{T}_n\right] |\Psi_T(\mathbf{R})\rangle$

The crucial challenge lies in extensively accounting for relatively small fluctuations in the electron charge densities. In FN-DMC this implies the need for relatively small time-steps $\Delta\tau$ for the projection of the wavefunction as well as an extensive sampling of electron configurations in real-space ($\lim_{\tau \rightarrow \infty}$) in order to reduce the stochastic noise in the predicted energy. In coupled cluster theory, non-covalent interactions require a high-order treatment of many-electron processes, as is included in CCSD(T), and a sufficiently large single-particle basis set. Reaching basis set saturation and well-controlled local approximations concurrently for the studied systems required previously unfeasible computational efforts as shown by the several kcal mol⁻¹ scatter of interaction energy predictions reported for the L7 set (see Fig. S3). Our recent efforts enabled the following: (i) a systematically converging series of local CCSD(T) results is presented for highly-complicated complexes, (ii) both the local and the basis set incompleteness (BSI) errors are closely monitored using comprehensive uncertainty measures [14], (iii) convergence up to chemical accuracy is reached for the complete L7 set concurrently in the local approximations as well as in the basis set saturation. The benefit of such demanding convergence studies is that the resulting interaction energies, up to the respective error bars, can be considered independent of the corresponding approximations. Consequently, we expect that the CBS limit of the exact CCSD(T) results could, in principle, be approached similarly using alternative basis sets [10, 30, 31] or local correlation methods [32–35], as it is clearly observed for some of the present complexes (see, *e.g.* GGG or CBH in Fig. S3).

We use highly-optimized algorithms both for FN-DMC and CCSD(T) as outlined in Methods, and push them beyond the typically applied limits. We used *circa* 0.7 and 1 million CPU core hours for FN-DMC and CCSD(T), respectively. This is equivalent to running a modern 28 core machine constantly for ~ 7 years.

Losing consensus on supramolecular interactions

Demonstrating agreement between fundamentally different electronic structure methods for solving the Schrödinger equation provides a proof-of-principle for the accuracy of the methods beyond technical challenges. To date, disagreements between CCSD(T) and FN-DMC have been reported only for systems where their key assumptions, *e.g.* single-reference wavefunction, accurate node-structure, etc. were not completely fulfilled [36, 37]. Previously however, CCSD(T) and FN-DMC were found in agreement within the error bars, for the interaction energies of small organic molecules with pure dynamic correlation [9, 16, 38] as well as some extended systems [11, 17, 39]. Establishing this agreement for systems at the 100 atom range has, however, been hindered by the sizable or unavailable error estimates for finite systems [9]. For example, binding energies of large host-guest complexes derived from experimental association free energies [40, 41] motivated previous FN-DMC [42] as well as local CCSD(T) [43] computations. However, conclusive remarks could not be made on the consistency of FN-DMC and local CCSD(T) on these complexes due to technical difficulties and unavailable uncertainty estimates for local CCSD(T), and large error estimates on both experimental and FN-DMC energies (up to a few kcal mol⁻¹).

Here, we consider similar but somewhat smaller supramolecular complexes (Fig. S2) and obtain tightly converged local CCSD(T) and FN-DMC results sufficient for rigorous comparisons (see Fig. S3 and Table SI). The level of uncertainty in our results is indicated by stochastic error bars for FN-DMC and the sum of local and BSI error estimates for CCSD(T). The complexes are arranged in Fig. S3 according to increasing interaction strength, which roughly scales with the size of the interacting surface. CCSD(T) and FN-DMC agree on the interaction energy to within 0.5 kcal mol⁻¹, taking error bars into account, for a subset of the complexes we consider: GGG, CBH, GCGC, C3A and PHE. These complexes are between 48 and 112 atoms in size and exhibit $\pi - \pi$ stacking, hydrogen bonding, and dispersion interactions. Therefore, the agreement for these five complexes indicates their absolute

interaction energies are established references and can be used to benchmark other methods for large molecules. Here, relative differences of very small interaction energies have to be interpreted carefully as they are sensitive to the uncertainty estimates. In GGG for example, Δ_{\min} is 0.1 kcal mol⁻¹ whilst the relative disagreement lies between 3% and 50%. In contrast, the relative disagreement between FN-DMC and CCSD(T) is better resolved in the more strongly interacting C₆₀@[6]CPPA complex, at 20–31%.

TABLE SI. Interaction energies in kcal mol⁻¹ for best estimated CCSD(T) and FN-DMC, as well as their minimum differences (Δ_{\min}) for the L7 supramolecular data set and the buckyball-ring complex (C₆₀@[6]CPPA). The indicated errors for CCSD(T) are extrapolated from the convergence of basis sets and local approximations in LNO-CCSD(T). The errors indicated in FN-DMC interaction energies are stochastic errors, with 1 standard deviation ($1-\sigma$).

Complex	No. of atoms	CCSD(T)	FN-DMC	Δ_{\min}
GGG	48	-2.1 ± 0.2	-1.5 ± 0.3	0.1
CBH	112	-11.0 ± 0.2	-11.4 ± 0.4	0.0
GCGC	58	-13.6 ± 0.4	-12.3 ± 0.3	0.5
C3A	87	-16.5 ± 0.8	-15.0 ± 0.5	0.2
C2C2PD	72	-20.6 ± 0.6	-18.1 ± 0.4	1.5
PHE	87	-25.4 ± 0.2	-26.5 ± 0.7	0.3
C3GC	101	-28.7 ± 1.0	-24.2 ± 0.7	2.9
C ₆₀ @[6]CPPA	132	-41.7 ± 1.7	-31.1 ± 0.7	8.3

A salient and surprising finding is the disagreement between state-of-the-art methods on the interaction energy of three non-trivial complexes: coronene dimer (C2C2PD), circumcoronene-GC base pair (C3GC), and buckyball-ring (C₆₀@[6]CPPA). Considering the error bars, the minimum differences (Δ_{\min}), as indicated in Table SI and Fig. S3 are 1.5, 2.9, and 8.3 kcal mol⁻¹ for C2C2PD, C3GC, and C₆₀@[6]CPPA, respectively, and could be as high as 3.5, 6.2, and 13.1 kcal mol⁻¹. Considering the comparable size of C3A, PHE, and CBH to C2C2PD, C3GC, and C₆₀@[6]CPPA, the Δ_{\min} values of the latter three complexes are not explained simply by the large size or the large area of the interacting surface. CCSD(T) predicts consistently stronger interaction in these complexes than FN-DMC, but at this point it is unclear what the exact interaction energies are.

C2C2PD has attracted the most attention to date in the CCSD(T) context as it represents a stepping stone between two widely studied systems: benzene dimer and graphene bilayer [9]. Already C2C2PD has posed a significant challenge to various local CCSD(T) methods due to its slowly-decaying long-range interactions [14, 33, 35, 44–47]. Considerable efforts have been devoted recently [14, 33, 35] to narrow down the local CCSD(T) interaction energy of C2C2PD to the range of about -19 to -21 kcal mol $^{-1}$. Thus the presently reported -20.6 ± 0.6 kcal mol $^{-1}$ interaction energy and previous local CCSD(T) results, containing analogous local approximations, consistently indicate stronger interaction than FN-DMC for C2C2PD.

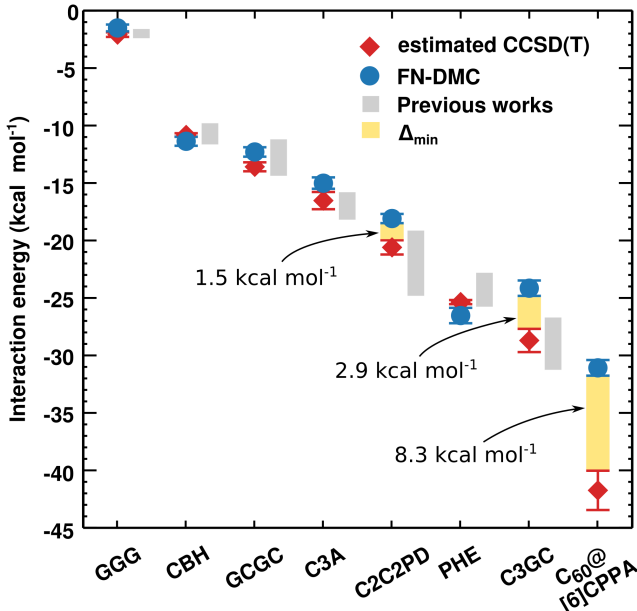


FIG. S3. CCSD(T) and FN-DMC interaction energies for the supramolecular complexes of the L7 data set [23] and the C₆₀@[6]CPPA buckyball-ring complex arranged in terms of increasing interaction strength. Gray bars mark the range of interaction energies reported in the literature using alternative wavefunction based methods [*e.g.* QCISD(T) [23], and various local CCSD(T) approaches [33, 35, 44–47]]. The yellow bars indicate the delta value (Δ_{\min}) which is the minimum difference between best converged CCSD(T) and FN-DMC, given by the estimated and stochastic error bars, respectively.

Distinct errors using DNA base molecules on circumcoronene

The C3GC and C3A complexes are ideal for assessing the convergence of CCSD(T) and FN-DMC, due to their chemical similarity and importance of $\pi - \pi$ stacking interactions, *i.e.* nucleobases stacked on circumcoronene. CCSD(T) and FN-DMC agree within 1 kcal mol⁻¹ for the interaction energy of C3A, whereas there is a notable disagreement of at least 2.9 kcal mol⁻¹ in the interaction energy of C3GC. Interestingly, both systems involve similar interaction mechanisms, with C3GC exhibiting both stacking and hydrogen-bonding interactions.

CCSD(T) and FN-DMC interaction energies involve multiple approximations. Known sources of error to consider in our FN-DMC calculations are:

- The fixed-node approximation which restricts the nodal-structure to that of the input guiding wavefunction.
- Time-step bias from the discretization of imaginary time for propagating the wavefunction.
- Pseudopotentials to approximate core electrons for each atom.
- Non-uniform quality of optimized trial wavefunctions for fragments and bound complex at larger time-steps.

In obtaining CCSD(T) interaction energies, the sources of error are:

- Local approximations of long-range electron correlation according to the LNO scheme.
- Single-particle basis representation of the CCSD(T) wavefunction.
- Neglected core electron correlation.
- Missing high-order many-electron contributions beyond CCSD(T).

In Fig. S4 we analyse the most critical approximations for each method on the example of the C3A and C3GC complexes, and we also consider the other remaining known sources of error in Methods.

For the single-particle basis representation in CCSD(T) we employed conventional correlation-consistent basis sets augmented with diffuse functions [48], aug-cc-pVXZ ($X=T$,

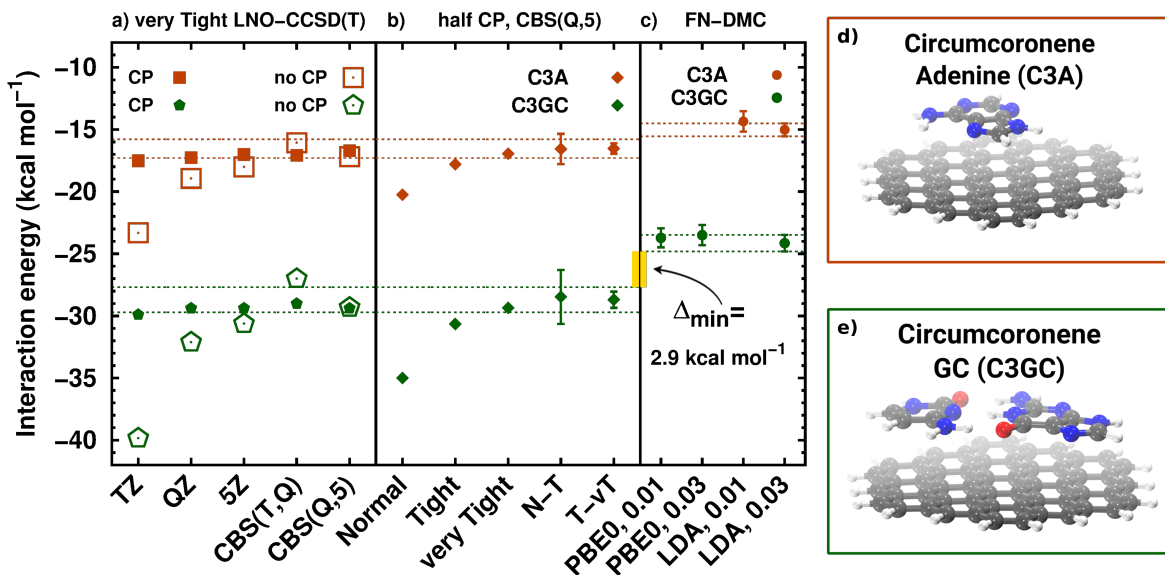


FIG. S4. The interaction energy of the C3A and C3GC complexes using LNO-CCSD(T) (panels a and b) and FN-DMC (panel c). The orange and green dashed horizontal lines, for C3A and C3GC, respectively, enclose the best estimated CCSD(T) (panel a and b) and the final FN-DMC (panel c) interaction energies using the corresponding uncertainty estimates and stochastic error bars. The FN-DMC error bars indicate a stochastic error of $1-\sigma$. The yellow bar denotes the minimum difference between CCSD(T) and FN-DMC (Δ_{\min}). (a) CP-corrected and uncorrected LNO-CCSD(T) interaction energies using the aug-cc-pVXZ basis sets, as well as CBS($X, X+1$) extrapolation. (b) Convergence of half CP-corrected LNO-CCSD(T)/CBS(Q,5) interaction energies using a series of LNO thresholds as well as Normal-Tight (N-T) and Tight-very Tight (T-vT) extrapolations. (c) FN-DMC interaction energies with two nodal surfaces for C3GC from DFT (PBE0 and LDA) and different time-steps (given in a.u.) for C3A and C3GC. (d) C3A complex. (e) C3GC complex.

Q, and 5) as shown in panel a) of Fig. S4. The remaining BSI is alleviated using extrapolation [49] toward the complete basis set (CBS) limit [CBS($X, X+1$), $X=T, Q$], and counterpoise (CP) corrections [50]. The local errors decrease systematically as the LNO threshold sets are tightened (Normal, Tight, very Tight) enabling extrapolations, *e.g.* Normal-Tight (N-T), to estimate the canonical CCSD(T) interaction energy [14] (see panel b) of Fig. S4). Exploiting the systematic convergence properties, an upper bound for both the local and the BSI errors can be given [51].

Benchmarks presented previously for energy differences of a broad variety of systems

showed excellent overall accuracy at the Normal–Tight extrapolated LNO-CCSD(T)/CBS(T,Q) level (M1) [14]. However, the BSI error bar of 1.0 kcal mol⁻¹ and the local error bar of 2.2 kcal mol⁻¹ obtained for C3GC at this M1 level are impractical for a definitive comparison with FN-DMC. The next steps along both series of approximations towards chemical accuracy, *i.e.* the use of very Tight LNO thresholds and the aug-cc-pV5Z basis set (M2), have been enabled by our recent method development efforts [13, 14, 52]. With these better converged interaction energies, the M2 level uncertainty estimates are up to a factor of three smaller than at the M1 level. Explicitly, 0.7 (0.4) kcal mol⁻¹ local (BSI) error estimate is obtained for C3GC. The same measures are the largest for C₆₀@[6]CPPA at the M2 level being 1.1 and 0.6 kcal mol⁻¹, respectively. Moreover, for the remaining L7 complexes, the local (BSI) uncertainty estimates indicate even better convergence of 0.1-0.4 (0.1-0.3) kcal mol⁻¹. Additional details are provided in Methods and in Section S1 of the Supplemental Material (SM).

FN-DMC has the advantage that the wavefunction is sampled in real-space without the need for the numerical representation of many-particle basis states thus reducing sensitivity to the single-particle basis set. Instead, pertinent sources of error in FN-DMC which we assess in Fig. S4 are the effects of the fixed-node approximation and the time-step bias. Note that these sources of error are not included in the FN-DMC stochastic error bars.

First, the different nodal surfaces from these DFT methods serve to indicate the dependence of the FN-DMC interaction energy on the nodal structure. Indeed, from Fig. S4, we find no indication that the FN-DMC interaction energies of C3GC is affected by the nodal structure outside of the stochastic error bars. Second, FN-DMC energies are sensitive to the time-step and we rely on recent improvements in FN-DMC algorithms [53, 54], that enable convergence of time-steps as large as 0.05 a.u. We used 0.03 a.u. and 0.01 a.u. time-steps to compute the interaction energies of C3A and C3GC. Fig. S4 indicates that the interaction energy is unchanged for C3A and C3GC (within the stochastic error) for the different time-steps considered here. The time-step and fixed-node approximations perform similarly well for the coronene dimer and the buckyball-ring complex (see Section S2 of the SM).

Open challenges for next generation of many-body methods

CCSD(T) and FN-DMC have been shown to agree with sub-chemical accuracy for small

organic dimers [9, 16, 38], molecular crystals [17], and small physisorbed molecules on surfaces [11, 39]. Indeed, we also find good agreement in the absolute interaction energies for five of the eight complexes considered here. However, we find that the disagreement by several kcal mol⁻¹ in C₆₀@[6]CPPA particularly, cannot be explained by the controllable sources of error. While both methods are highly sophisticated, they are still approximations to the exact solution of the many-electron Schrödinger equation. Moreover, there can be non-trivial coupling between approximations within each method, which remain poorly understood for complex many-electron wavefunctions. Here, we estimate the magnitude of additional approximations which are generally regarded as even more robust and contemplate potential strategies for improvements.

1. *Are we there yet with FN-DMC?*

The reported interaction energies of C2C2PD, C3GC, and C₆₀@[6]CPPA indicate that FN-DMC stabilizes the interacting complexes more weakly than CCSD(T). Therefore, one possibility for the discrepancy between the methods is that FN-DMC (as applied here) does not capture the correlation energy in the bound complexes sufficiently. Reasons for this can include the fixed-node approximation and more generally, insufficient flexibility in the wavefunction ansatz.

The Slater-Jastrow ansatz was applied here using a single determinant combined with a Jastrow factor containing explicit parameterizable functions to describe electron-electron, electron-nucleus, and electron-electron-nucleus interactions. We have evaluated FN-DMC interaction energies for different nodal structures for C3GC, C2C2PD, C₆₀@[6]CPPA and in all cases the FN-DMC interaction energies are in 1- σ agreement (see Section S2 of SM) with stochastic errors that are mostly under 1 kcal mol⁻¹. Among these systems, the largest potential deviation (Δ_{\max}) due to the fixed-node error is estimated to be ~ 3.7 kcal mol⁻¹ in C₆₀@[6]CPPA. Although this potentially large source of error is not enough to explain the 8.3 kcal mol⁻¹ Δ_{\min} disagreement with CCSD(T), it remains a pertinent issue for establishing chemical accuracy. Reducing the fixed-node error, for example by using more than one Slater determinant to systematically improve the nodal structure, in such large molecules remains challenging [55, 56]. Promising alternatives include the Jastrow antisymmetrized geminal power approach which has recently been shown to recover near-exact results for a

small, strongly correlated cluster of hydrogen atoms [57].

The Jastrow factor is a convenient approach to increase the efficiency of FN-DMC since in the zero time-step limit and with sufficient sampling, the FN-DMC energy is independent of this term. However, the quality of the Jastrow factor can be non-uniform for the bound complex and the non-interacting fragments, which can introduce a bias at larger time-steps. The recent DLA method in FN-DMC reduces this effect [54] and was applied to the $C_{60}@[6]CPPA$ complex reported in Table SI and also tested for GGG, C3A, and C2C2PD complexes (see Methods for further details). In all cases, FN-DMC with DLA is in decent agreement (within $1-\sigma$) with non-DLA FN-DMC interaction energies. For example, the C2C2PD FN-DMC interaction energy with DLA is -17.4 ± 0.5 kcal mol $^{-1}$ whilst with standard LA, it is -18.1 ± 0.4 kcal mol $^{-1}$. Moreover, the interaction strengths tend towards being weaker with DLA in the systems we consider, *i.e.* further from the CCSD(T) interaction energies. As such, the discrepancy between FN-DMC and CCSD(T) remains regardless of any potential error from the Jastrow factor in our findings.

We estimate the error from the use of Trail and Needs pseudopotentials [58, 59] in FN-DMC at the Hartree-Fock (HF) level using interaction energy of C2C2PD. We find 0.1 kcal mol $^{-1}$ difference in the HF interaction energy with the employed pseudopotentials and without (*i.e.* all-electron) which is well within the acceptable uncertainty for our findings. In addition, Zen *et al.* [17] have previously compared Trail and Needs pseudopotentials with correlated electron pseudopotentials [60] at the FN-DMC level using the binding energy of an ammonia dimer and found agreement within 0.1 kcal mol $^{-1}$.

In principle, a more flexible wavefunction ansatz allows a more accurate many-body wavefunction to be reached in DMC, thus recovering electron correlation more effectively. To this end, recently introduced machine learning approaches [61, 62] are promising but more expensive due to the considerable increase in parameters. However once feasible, a systematic assessment of the amount of electron correlation recovered by these different ansatze in non-covalently bound systems will bring valuable insight to the current puzzle.

2. Potential avenues for improvement upon CCSD(T)

Considering the complexes exhibiting significant $\pi-\pi$ interactions, CCSD(T) is found to predict stronger interaction than FN-DMC. As some of the individually negligible but

collectively important long-range interactions are estimated in local CC methods, these potentially overestimated interaction energy contributions could benefit from a higher-level theoretical description [33, 63]. In the case of the LNO scheme, the majority of the local approximations have marginal effect on the interaction energies when very Tight settings are employed [14]. For instance, long-range interactions that do not benefit from the full CCSD(T) treatment add up to at most 2.9 kcal mol⁻¹ for the interaction energy of C₆₀@[6]CPPA. The presented error estimate allowing for almost 40% error in this term reliably covers this approximation. While these and other non-negligible LNO approximations are closely monitored (see Section S1 A of SM), remaining uncertainties outside of the presented error bars cannot be ruled out. All in all, the convergence measures assessing the local errors of LNO-CCSD(T) interaction energies indicate at least 97.4% or 1.1 kcal mol⁻¹ certainty.

The employed single-particle basis sets perform exceptionally well for CCSD(T) computations of small molecules [48, 49], but approaching the CBS limit of CCSD(T) for large systems is mostly an uncharted territory in the literature [14, 33]. The agreement of CP corrected CBS(T,Q), CBS(Q,5), and uncorrected CBS(Q,5) within 0.06–0.36 kcal mol⁻¹ is highly satisfactory (see Sect. S1 B of SM). Furthermore, the CBS(5,6) results obtained with the aug-cc-pV6Z basis set for GGG are fully consistent with the CBS(Q,5) interaction energies (see Sect. S1 B of SM). CC methods exploiting explicitly correlated wavefunction forms [33, 35] as well as alternatives to the conventional Gaussian basis sets [10, 30, 31] have emerged recently, which could provide independent verification of the systematic convergence studies performed here.

The higher-order contribution of three-, four-, etc. electron processes on top of CCSD(T) are usually found to be negligible for weakly-correlated molecules [38]. However, the available numerical experience is limited to complexes below about a dozen atoms, and for some highly polarizable systems the beyond CCSD(T) treatment of three-electron processes has been shown to contribute significantly to three-body dispersion [64]. The weakly-correlated nature of all complexes is indicated by that the perturbative (T) contribution to the total correlation energy component of the CCSD(T) interaction energy is consistently around 18–20%. Additionally, the CC amplitude based measures all point to pure dynamic correlation. According to our LNO approximated estimations for the GGG complex, the infinite-order three-electron terms on top of the perturbative treatment of (T) is

only about $-0.01 \text{ kcal mol}^{-1}$, while the perturbative four-electron contribution [65] is around $-0.02 \text{ kcal mol}^{-1}$ (see Sect. S1 D of SM). Due to the extreme computational cost of such computations, it remains an open and considerable challenge to establish, on a representative sample size, whether the contribution of higher-order processes is within sub-chemical accuracy for larger and more complex molecules.

The effect of core correlation is expected to be very small, thus we attempted to evaluate it independently from the numerical noise of the other approximations. For instance, the all electron interaction energy of C2C2PD is even stronger than the frozen core one at second-order by $0.2 \text{ kcal mol}^{-1}$ (4.6 cal mol^{-1} per C atom). All in all, core and higher-order correlation effects appear to strengthen the CCSD(T) interaction energies and slightly increase the deviation compared to FN-DMC.

3. *Insights from experiments and density-functional approximations*

Experimental binding energies or association constants of supramolecular complexes are particularly valuable, when available, but also have their limitations as back-corrections are needed to separate the effects of thermal fluctuations and solvent effects for example [66]. In the case of $\text{C}_{60}@[6]\text{CPPA}$ for example, the association constant is measured in a benzene solution and indicates a stable encapsulated complex, but one which could not be well-characterised by X-ray crystallography; purportedly due to the rapid rotation of the buckyball guest [67]. Instead, a non-fully encapsulated structure was successfully characterized using toluene anchors on the buckyball. This demonstrates a number of physical leaps that exist between what can be measured and what can be accurately computed.

Other high-level methods, such as the full configuration interaction quantum Monte-Carlo (FCI-QMC) method [10, 30], can be key to assessing the shortcomings from major approximations such as the fixed node approximation and static correlation. Once the severe scaling with system size associated with FCI-QMC and similar methods is addressed, larger molecules will become feasible. However, in the present time the lack of references in large systems remains a salient problem.

The scarcity of reference information has an impact on all other modelling methods, including density-functional approximations (DFAs), semi-empirical, force field or machine learning based models, etc. which are validated or parameterized based on higher-level

benchmarks. In particular, there is a race to simulate larger, more anisotropic, and complex materials, accompanied by a difficulty of choice for modelling methods. To demonstrate the consequences of inconsistent references, Fig. S5 shows interaction energy discrepancies obtained with DFAs, PBE0+D4 [26] and PBE0+MBD [27], that are both designed to capture all orders of many-body dispersion interactions in different manner. Intriguingly, the PBE0+D4 method is in close agreement with CCSD(T) (mean absolute deviation, MAD=1.1 kcal mol⁻¹), whereas PBE0+MBD is closer to FN-DMC (MAD=1.5 kcal mol⁻¹), but their performance is hard to characterize when CCSD(T) and FN-DMC disagree. Moreover, we decomposed the interaction energies from the DFAs into dispersion components and find that, for C₆₀@[6]CPPA the main difference between PBE0+MBD and PBE0+D4 is 6.5 kcal mol⁻¹ in the two-body dispersion contribution. Differences in beyond two-body dispersion interactions are smaller and at most 1.6 kcal mol⁻¹ in C₆₀@[6]CPPA.

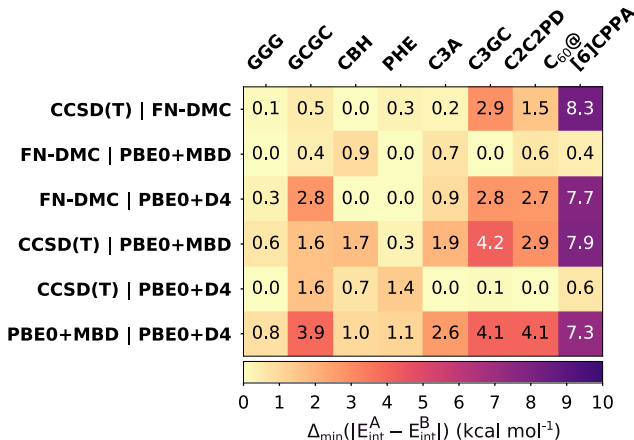


FIG. S5. $\Delta_{\min}(|E_{\text{int}}^{\text{A}} - E_{\text{int}}^{\text{B}}|)$ is shown which is the smallest absolute difference in E_{int} between pairs of methods ($|E_{\text{int}}^{\text{A}} - E_{\text{int}}^{\text{B}}|$) in kcal mol⁻¹, with methods A and B indicated along the vertical axis. Δ_{\min} takes into account the error estimates for CCSD(T) and FN-DMC to show smallest possible differences with respect to these reference methods. The DFT methods have no quantified uncertainty estimates associated with them. The compared methods are: CCSD(T), FN-DMC, PBE0+MBD and PBE0+D4. The supramolecular complexes are those in the L7 data set and the C₆₀@[6]CPPA buckyball-ring complex.

DISCUSSION

Until now, disagreements between reference interaction energies of extended organic complexes have typically been ascribed to unconverged results due to practical bottlenecks. Here, we report highly-converged results at the frontier of wavefunction based methods; uncovering a disconcerting level of disagreement in the interaction energy for three supramolecular complexes. We have computed interaction energies from CCSD(T) and FN-DMC for a set of supramolecular complexes of up to 132 atoms exhibiting challenging intermolecular interactions. The accuracy of these methods have been repeatedly corroborated in the domain of dozen-atom systems with single-reference character and here we find CCSD(T) and FN-DMC are in excellent agreement for five of the supramolecular complexes suggesting that these methods are able to maintain remarkable accuracy in some larger molecules. However, FN-DMC and CCSD(T) interaction energies disagree by 1.5 kcal mol⁻¹ in the coronene dimer (C2C2PD), 2.9 kcal mol⁻¹ in GC base pair on circumcoronene (C3GC) and 8.3 kcal mol⁻¹ in a buckyball-ring complex (C₆₀@[6]CPPA). These disagreements are cemented by reporting sub-kcal mol⁻¹ stochastic errors in FN-DMC and a systematically converging series of local CCSD(T) interaction energies accompanied by uncertainty estimates approaching chemical accuracy. Therefore, despite our best efforts to suppress all controllable sources of error, the marked disagreement of FN-DMC and CCSD(T) prevents us from providing conclusive reference interaction energies for these three complexes. Such large differences in interaction energies surpass the widely-sought 1 kcal mol⁻¹ chemical accuracy and indicate that the highest level of caution is required even for our most advanced tools when employed at the hundred-atom scale.

The supramolecular complexes we report feature $\pi - \pi$ stacking, hydrogen bonding, and intermolecular confinement, that are ubiquitous across natural and synthetic materials. Thus our immediate goals are to elucidate the sources of the underlying discrepancies and to explore the scope of systems where such deviations between reference wavefunction methods occur. Well-defined reference interaction energies and the better characterization of their predictive power have growing importance as they are frequently applied in chemistry, material, and biosciences. Our findings should motivate cooperative efforts between experts of computational and experimental methods in obtaining well-defined interaction energies and thereby extending the predictive power of first principles approaches across the board.

METHODS

The L7 structures have been defined by Sedlak *et al.* [23] and structures can be found on the begdb database [68]. Note that the interaction energy, E_{int} , is defined with respect to two fragments even where the complex consists of more than two molecules (as in GGG, GCGC, PHE, and C3GC):

$$E_{\text{int}} = E_{\text{com}} - E_{\text{frag}}^1 - E_{\text{frag}}^2 \quad (1)$$

where E_{com} is the total energy of the full complex, and E_{frag}^1 and E_{frag}^2 are the total energies of isolated fragments 1 and 2, respectively. The fragment molecules have the same geometry as in the full complex, *i.e.* not relaxed. Further details on the configurations can be found in the SM and in Ref. 23.

The $\text{C}_{60}@[6]\text{CPPA}$ complex is based on similar complexes in previous theoretical and experimental works [42, 69, 70] and has been chosen to represent confined π - π interaction that are numerically still tractable by our methodologies. Its geometry has been symmetrized to D_{3d} point group, the individual fragments of C_{60} and [6]CPPA are kept frozen (I_h and D_{6h} , respectively). The structure is provided in the SM.

The local natural orbital CCSD(T) method

In order to reduce the N^7 -scaling of canonical CCSD(T) with respect to the system size (N), the inverse sixth power decay of pairwise interactions can be exploited (local approximations) and the wavefunction can be compressed further via natural orbital (NO) techniques. [63] Building on such cost-reduction techniques a number of highly-efficient local CCSD(T) methods emerged in the past decade [13, 14, 32–35, 63]. As the local approximation free CCSD(T) energy can be approached by the simultaneous improvement of all local truncations in most of these techniques, in principle, all local CCSD(T) methods are expected to converge to the same interaction energy. Here we employ the local natural orbital CCSD(T) [LNO-CCSD(T)] scheme [13, 71], which, for the studied systems, brings the feasibility of exceedingly well-converged CCSD(T) calculations in-line with FN-DMC. The approximations of the LNO scheme automatically adapt to the complexity of the underlying wavefunction and enable systematic convergence towards the exact CCSD(T) correlation energy, with up to 99.99% accuracy using sufficiently tight settings [14].

The price of improvable accuracy is that the computational requirements can drastically increase depending on the nature of the wavefunction: while LNO-CCSD(T) has been successfully employed for macromolecules, such as small proteins at the 1000 atom range [13, 14], sizable long-range interactions appearing in the here studied complexes pose a challenge for any local CCSD(T) method [14, 32, 33, 35]. This motivated the implementation of several recent developments in our algorithm and computer code over the lifetime of this project, which cumulatively resulted in about 2-3 orders of magnitude decrease in the time-to-solution and data storage requirement of LNO-CCSD(T) [13, 14, 71], and made well-converged computations feasible for all complexes. For instance, we have designed a massively parallel conventional CCSD(T) code specifically for applications within the LNO scheme [72] and integrated it with our highly optimized LNO-CCSD(T) algorithms [13, 14, 71]. Here, we report the first large-scale LNO-CCSD(T) applications which exploit the resulted high performance capabilities using the most recent implementation of the MRCC package [52] (release date February 22, 2020).

Computational details for CCSD(T)

The LNO-CCSD(T)-based CCSD(T)/CBS estimates were obtained as the average of CP-corrected and uncorrected (“half CP”) [50], Tight–very Tight extrapolated LNO-CCSD(T)/CBS(Q,5) interaction energies [14]. Except for C3A, C3GC, and C₆₀@[6]CPPA, the CBS(Q,5) notation refers to CBS extrapolation [49] using aug-cc-pVXZ basis sets [48] with $X=Q$ and 5. For C3A, C3GC, and C₆₀@[6]CPPA, a Normal LNO-CCSD(T)/CBS(Q,5)-based BSI correction (Δ_{BSI}) was added to the Tight–very Tight extrapolated LNO-CCSD(T)/aug-cc-pVTZ interaction energies, exploiting the parallel convergence of the LNO-CCSD(T) energies for these basis sets [14]. Local error bars shown, *e.g.* on panel b) of Fig. S4 are obtained via the extrapolation scheme of Ref. [14]. Error bars accompanying the LNO-CCSD(T) interaction energies of Fig. S3 and Table SI, and determining the interval enclosed by the dashed lines on panels a) and b) of Fig. S4 are the sums of the BSI and local error estimates. The BSI error measure is the maximum of two separate error estimates: the difference between CP-corrected and uncorrected CBS(Q,5) energies, and the difference between CP-CBS(T,Q) and CP-CBS(Q,5) results. This BSI error bar is increased with an additional term if Δ_{BSI} is employed according to Sect. S1 B of the SM. The local error

bar of the best estimated CCSD(T) results (see Table SII of the SM) is obtained from the difference of the Tight and very Tight LNO-CCSD(T) results evaluated with the largest possible basis sets [14].

Computational details for FN-DMC

Our FN-DMC calculations use the Slater-Jastrow ansatz with the single Slater determinants obtained from DFT. The Jastrow factor for each system contains explicit electron-electron, electron-nucleus, and three-body electron-electron-nucleus terms. The parameters of the Jastrow factor were optimized for each complex using the variational Monte Carlo (VMC) method and the varmin algorithm which allows for systematic improvement of the trial wavefunction, as implemented in CASINO v2.13.610 [73]. Note that bound complexes were used in the VMC optimizations and the resulting Jastrow factor was used to compute the corresponding fragments. All systems were treated in real-space as non-periodic open systems in VMC and FN-DMC.

We performed FN-DMC with the locality approximation (LA) for the non-local pseudopotentials [74] and 0.03 a.u. time-step for all L7 complexes. Smaller time-steps of 0.003 and 0.01 a.u. were also used to compute the interaction energy of the C2C2PD complex and the interaction energy was found to be in agreement within the stochastic error bars with all three time-steps.

The $C_{60}@[6]CPPA$ complex exhibited numerical instability using the standard LA. This prevented sufficient statistical sampling and therefore we computed this complex with two alternative and more numerically stable approaches. First, the energy reported in Fig. S3 and Table SI is using the recently developed determinant localization approximation (DLA) [54] implemented in CASINO v2.13.809 [73]. The DLA gives: (i) better numerical stability than the LA algorithm allowing for more statistics to be accumulated, (ii) smaller dependence on the Jastrow factor, and (iii) addresses an indirect issue related to the use of non-local pseudopotentials. Second, the T-move approximation [75] (without DLA) was also applied to $C_{60}@[6]CPPA$ for comparison. The T-move scheme is more numerically stable than the standard LA algorithm but is also more time-step dependent and therefore we used results from 0.01 and 0.02 a.u. time-steps to extrapolate the interaction energy to the zero time-step limit, as reported in SM. The extrapolated interaction energy with the T-move scheme is

-31.14 ± 2.57 kcal mol⁻¹ using LDA nodal structure and -29.16 ± 2.33 kcal mol⁻¹ using PBE0 nodal structure. Due to the large stochastic error on these results, we report the better converged DLA-based interaction energy (with PBE0 nodal structure) in the main results, but we note that all three predictions from FN-DMC agree within the statistical error bars. Furthermore, as the DLA is less sensitive to the Jastrow factor at finite time-steps, we have also tested the interaction energies of GGG, C3A, and C2C2PD complexes, finding agreement with the LA-based FN-DMC results within one standard deviation. Further details can be found in the SM.

The initial DFT orbitals (which define the nodal structure in FN-DMC) were prepared using PWSCF in Quantum Espresso v.6.1 [76]. Trail and Needs pseudopotentials [58, 59] were used for all elements, with a plane-wave energy cut-off of 500 Ry. The plane-wave representation of the molecular orbitals from PWSCF were expanded in terms of B-splines. Since PWSCF uses periodic boundary conditions, all complexes were centered in an orthorhombic unit cell with a vacuum spacing of ~ 8 Å in each Cartesian direction to ensure that the single-particle orbitals are fully enclosed. LDA orbitals were used for L7 complexes and in addition, PBE0 orbitals were also considered for C2C2PD, C3GC, and C₆₀@[6]CPPA. In all cases, the final FN-DMC interaction energy from LDA and PBE0 nodal structures are in agreement within the stochastic errors.

ACKNOWLEDGMENTS

We thank Dr. Andrea Zen for discussions. We thank HPC staff for their support and access to the IRIS cluster at the University of Luxembourg and to the DECI resource Saga based in Norway at Trondheim with support from the PRACE aisbl (NN9914K). **Funding:** YSA thanks funding from NIH grant number R01GM118697 and is supported by The National Centre of Competence in Research (NCCR) Materials Revolution: Computational Design and Discovery of Novel Materials (MARVEL) of the Swiss National Science Foundation (SNSF). The work of PRN is supported by the ÚNKP-19-4-BME-418 New National Excellence Program of the Ministry for Innovation and Technology and the János Bolyai Research Scholarship of the Hungarian Academy of Sciences. JGB acknowledges support from the Alexander von Humboldt foundation. MK is grateful for the financial support from the National Research, Development, and Innovation Office (NKFIH, Grant No. KKP126451)

and the BME-Biotechnology FIKP grant of EMMI (BME FIKP-BIO). AT acknowledges financial support from the European Research Council (ERC-CoG grant BeStMo).

AUTHOR CONTRIBUTIONS

YSA and PRN contributed equally to this work. Major *investigation* was conducted by PRN (performing coupled cluster calculations) and YSA (performing quantum Monte Carlo calculations). JGB performed PBE0+D4 calculations and supporting validation calculations. DB performed PBE0+MBD calculations. The work has been *conceptualized* by YSA and AT with additional contribution from JGB and PRN. *Software development* to expand the application of LNO-CCSD(T) method in this work has been conducted by PRN and MK. PRN performed *formal analysis* to obtain uncertainty estimates from LNO-CCSD(T) data. The *original draft* of the manuscript was written by YSA and PRN. Additional *review and editing* of the manuscript was undertaken by JGB, AT, and MK. *Project administration* was led by YSA with contribution from JGB and AT. JGB and AT supervised the work.

SUPPLEMENTAL MATERIAL

CONTENTS

Main	3
State-of-the-art methods for non-covalent interactions	7
Losing consensus on supramolecular interactions	8
Distinct errors using DNA base molecules on circumcoronene	11
Open challenges for next generation of many-body methods	13
1. Are we there yet with FN-DMC?	14
2. Potential avenues for improvement upon CCSD(T)	15
3. Insights from experiments and density-functional approximations	17
Discussion	19
Methods	20
The local natural orbital CCSD(T) method	20
Computational details for CCSD(T)	21
Computational details for FN-DMC	22
Acknowledgments	23
Supplemental Material	25
S1. Details of CCSD(T) computations	26
A. Convergence of local approximations	26
B. Single-particle basis set convergence	30
C. LNO-CCSD(T) energies plotted on Figs. S4. and S6	33
D. Core and higher-order correlation on top of CCSD(T)	37
S2. Details of Quantum Monte Carlo calculations	38
A. Variational Monte Carlo Optimization of the Jastrow Factor	38
B. Time-Step and Node-Structure Dependence of the Coronene Dimer	40
C. The GGG Trimer and Coronene Dimer with the Determinant Localization Approximation	40

D. FN-DMC with T-move on the C ₆₀ @[6]CPPA Complex	41
S3. Computational requirements of LNO-CCSD(T) and FN-DMC	42
S4. Details of DFT calculations	44
S5. Geometry of the L7 and the C ₆₀ @[6]CPPA complexes	44
References	48
Author contributions	24

S1. DETAILS OF CCSD(T) COMPUTATIONS

Definitions:

- Interaction energy: according to the Methods Section of the main text, the difference of the complex’s energy consisting of all molecules and of the two subsystem energies, using unrelaxed structures for the latter. Notation: $E_Y^{\text{LNO-CCSD(T)}}[\text{aug-cc-pVXZ}]$, where Y refers to the level of local approximations (*Normal*, *Tight*, or *very Tight*) and X labels the cardinal number of the basis set.
- counterpoise (CP) corrected interaction energy: the energy of the subsystems are evaluated for the interaction energy expression using all single-particle basis functions of the complete complex including basis functions residing on the atomic positions of the other subsystem.
- local error bar: difference of the Tight and very Tight LNO-CCSD(T) results evaluated with the largest possible basis set.
- basis set incompleteness (BSI) error bar: maximum of two BSI error indicators, which are the difference of the CP corrected and uncorrected LNO-CCSD(T)/CBS(Q,5) interaction energies, and the difference of CP corrected LNO-CCSD(T)/CBS(T,Q) and LNO-CCSD(T)/CBS(Q,5) interaction energies.

A. Convergence of local approximations

The LNO-CCSD(T) energy expression reformulates the CCSD(T) energy in terms of localized molecular orbitals (LMOs, i', j') [13, 71, 77]:

$$E^{\text{LNO-CCSD(T)}} = \sum_{i'} \left[\delta E_{i'}^{\text{CCSD(T)}} + \Delta E_{i'}^{\text{MP2}} + \frac{1}{2} \sum_{j'}^{\text{distant}} \delta E_{i'j'} \right]. \quad (2)$$

The correlation energy contribution of distant LMO pairs is obtained at the level of approximate MP2 [13, 78] (third term), while all remaining LMO-pairs contribute to the CCSD(T) level treatment (first term). For the latter, first, local natural orbitals (LNOs) are constructed individually for each LMO at the MP2 level using a large domain of atomic and correlating (virtual) orbitals surrounding the LMO. The $\delta E_{i'}^{\text{CCSD(T)}}$ contribution is then computed in this compressed LNO orbital space, while the second term of Eq. (2) represents a correction for the truncation of the LNO space at the MP2 level of theory.

The convergence of all approximations in LNO-CCSD(T) can be assessed via the use of pre-defined threshold sets, which provide systematic improvement simultaneously for all approximations of the LNO scheme [13, 14, 71, 77–80]. In this series of threshold sets (*Normal*, *Tight*, *very Tight*), the accuracy determining cutoff parameters are tightened in an exponential manner [14]. For instance, the *very Tight* set collects an order of magnitude tighter truncation thresholds than those of the *Normal* set, which is the default choice. The convergence behavior of the LNO-CCSD(T) interaction energies separates the studied complexes (see Fig. 2 of manuscript) into two groups. For GGG, PHE, CBH, and GCGC we observe rapid convergence toward the corresponding canonical CCSD(T) interaction energy as indicated, *e.g.* by the local error estimates collected in Table SII. The excellent convergence is apparent as the differences of the *Tight* and *very Tight* interaction energies are all in the 0.1-0.3 kcal mol⁻¹ range for these four complexes. This uncertainty range is highly satisfactory for the local approximations considering that the estimated basis set incompleteness (BSI) errors for LNO-CCSD(T) are also comparable.

TABLE SII. Best converged [*Tight-very Tight* extrapolated LNO-CCSD(T)/CBS(Q,5) based] CCSD(T) interaction energies (IEs) and corresponding error estimates with full, half, and no CP correction. Our best estimates are highlighted in bold and are used throughout the manuscript.

System:	GGG	CBH	GCGC	C3A	C2C2PD	PHE	C3GC	C ₆₀ @[6]CPPA
IE, no CP	-1.98	-10.93	-13.38	-16.79	-20.36	-25.34	-28.67	-41.60
IE, CP	-2.20	-11.10	-13.80	-16.28	-20.84	-25.38	-28.73	-41.89
IE, half CP	-2.09	-11.01	-13.59	-16.53	-20.60	-25.36	-28.70	-41.74
Local error	0.09	0.10	0.16	0.42	0.38	0.07	0.65	1.10
BSI error	0.11	0.06	0.22	0.24	0.24	0.12	0.19	0.36
Δ_{BSI} error				0.10			0.17	0.25
Total error	0.20	0.15	0.39	0.75	0.62	0.18	1.01	1.71

Consequently, we perform an even more thorough analysis of the local errors for the remaining four complexes, C2C2PD, C3A, C3GC, and C₆₀@[6]CPPA, where the local error estimate of the LNO-CCSD(T) interaction energies is larger than 0.3 kcal mol⁻¹. The convergence pattern with *Normal*, *Tight*, and *very Tight* settings of the C3A and C3GC interaction energies is shown on the panel b) of Fig. S4 of the main text. The monitored convergence is monotonic and the remaining local error is about halved in each step, as observed for multiple systems previously [14] as well for the above four complexes. Additionally, the *Normal-Tight* and the *Tight-very Tight* based CCSD(T) estimates (data points with error bars on panel b) of Fig. S4 of the main text) agree closely, and the *Tight-very Tight* error bars are enveloped by the *Normal-Tight* ones. The same trends can be observed in Fig. S6 for the coronene dimer, where LNO-CCSD(T) interaction energies are collected with all investigated basis sets and all three LNO threshold combinations. Again, the convergence patterns with the improving local approximations are parallel for all basis sets, the *Normal-Tight* and *Tight-very Tight* estimates agree within 0.5 kcal mol⁻¹, and the *Tight-very Tight* error bars are 2-3 times narrower. Although, in the case of C₆₀@[6]CPPA, the *Normal* to *very Tight* series is only available with the aug-cc-pVTZ basis set, the 0.2 kcal mol⁻¹ agreement of *Normal-Tight* and the *Tight-very Tight* based CCSD(T) estimates and the threefold improvement provided by the *Tight-very Tight* error bar over the *Normal-Tight* one illustrate

analogous behavior to the cases of C2C2PD, C3A, and C3GC.

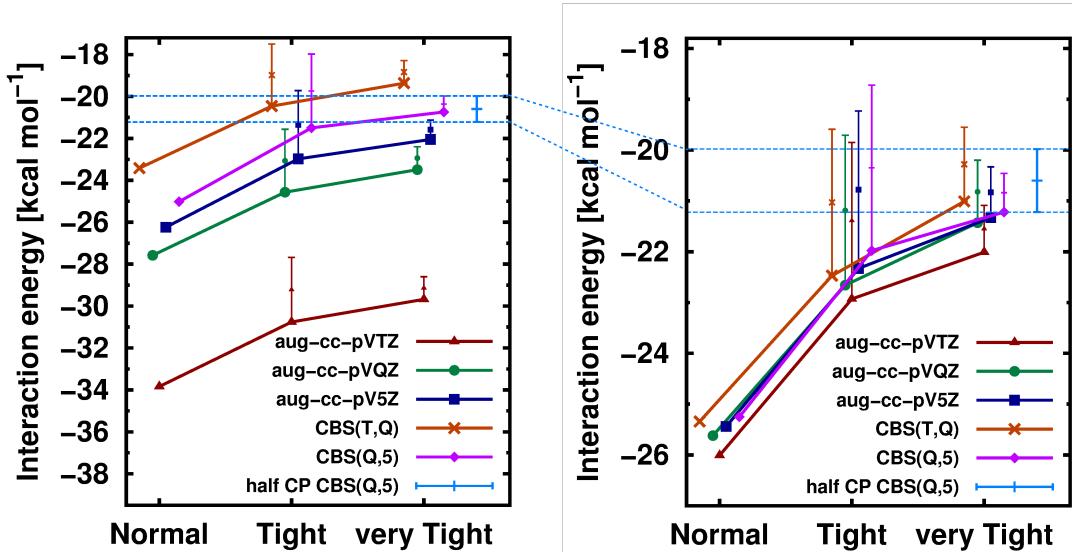


FIG. S6. Convergence of LNO-CCSD(T) interaction energies for the C2C2PD complex with various basis sets and LNO threshold sets. The left (right) panel collects results obtained without (with) CP correction. The *Normal–Tight* and the *Tight–very Tight* extrapolated results are plotted with a smaller point size also at the *Tight* and *very Tight* x axis labels, respectively, and they are accompanied by error bars indicating the uncertainty estimate of the local approximations at that level. For comparison the best CCSD(T)/CBS estimate [Tight-very Tight approximated, half CP corrected LNO-CCSD(T)/CBS(Q,5)] result and its corresponding uncertainty estimate is depicted on both panels via the light blue error bars and dashed horizontal lines. Note the different y ranges of the two panels as highlighted by dashed blue lines connecting the two panels. Also note that symbols corresponding to a given basis set are slightly shifted along the x-axis to improve visibility for all data points.

Considering briefly the corresponding absolute energies collected in Sect. S1 C, one can observe that the LNO-CCSD(T) correlation energies are also sufficiently well converged. For instance, for the C3GC complex *very Tight* based results provide four (almost five) converged significant digits in the correlation energies, which is then reliably translates into the observed cca. $0.65 \text{ kcal mol}^{-1}$ local uncertainty of the LNO-CCSD(T) interaction energies.

One can also consider internal convergence indicators besides the total energy. At the very Tight level, the $\pi-\pi$, $\pi-\sigma$, and also the majority of the $\sigma-\sigma$ orbital interactions benefit from

the full CCSD(T) treatment for all complexes. Additionally, none of the remaining weak electronic interactions, contributing only about 0.01% or lower portion of the correlation energy, are neglected, they are, however, approximated via second-order pair energies [13, 14]. At the very Tight level, the orbital domains employed for the LNO-CCSD(T) treatment include all atoms, all atomic orbitals, and the majority of the correlating (virtual) space, spanned by, on the average, 80–95% of the orbitals of the entire complexes.

B. Single-particle basis set convergence

Regarding the convergence of the interaction energies with respect to the single particle basis set, we rely on approaches used routinely in wavefunction computations on small molecules. Dunning’s correlation consistent basis sets [48] employed here are designed to systematically approach the complete basis set (CBS) limit with a polynomial convergence rate, which can be exploited to reduce the remaining basis set incompleteness (BSI) error via basis set extrapolation approaches [49, 81]. We employ two-point formulae for extrapolation, labeled as CBS($X, X + 1$), where X refers to the cardinal number of the aug-cc-pV X Z basis set [48] with $X=T, Q,$ and 5.

For the proper description of important medium- and long-range interactions and of the cross-polarization of the monomers in the complex, it is crucial to employ diffuse, i.e., spatially spread basis functions. The use of such diffuse basis functions, however, greatly enhances technical challenges characteristic of interaction energy computations with atom centered Gaussian type basis functions. As long as the basis set expansion of the monomers is not saturated completely, the basis functions residing on the atoms of one monomer can contribute to the description of the wavefunction components of the other monomer. Thus, the resulting basis set superposition error (BSSE) emerges from the unbalanced improvement of the basis set expansion of the monomers and the dimer and usually leads to artificially overestimated interaction strength. The BSSE can be decreased significantly by counterpoise (CP) corrections [50], i.e., by using the entire dimer basis set also for the monomer calculations. Naturally, for small basis sets this approach might lead to a more saturated basis set expansion on the monomers and can potentially overcorrect the BSSE. In the case of aug-cc-pV X Z with $X=T, Q,$ and 5 the CP correction decreases monotonically with increasing basis set size, thus a decreasing CP correction is an excellent indicator of basis set

saturation, which we employ here.

To characterize the convergence of the LNO-CCSD(T) interaction energies in terms of the basis set completeness, the maximum of two BSI error indicators is considered with the best available LNO threshold set. One of them is the difference of the CP corrected and uncorrected LNO-CCSD(T)/CBS(Q,5) interaction energies, and the other one is the difference of CP corrected LNO-CCSD(T)/CBS(T,Q) and LNO-CCSD(T)/CBS(Q,5) interaction energies. The resulting BSI error bar values of Table SII indicate that the above two four-membered groups exhibit much more homogeneous basis set convergence behavior. For the GGG, GCGC, PHE, and CBH interaction energies, this BSI measure is 0.06-0.22 kcal mol⁻¹, while for the other four complexes a twice as large uncertainty of 0.19-0.36 kcal mol⁻¹ is found. Compared to the similar or larger local error bars, we find this level of basis set convergence to be highly satisfactory.

We again investigate more closely only the C3A, C3GC, C2C2PD, and C₆₀@[6]CPPA quartet. The convergence of LNO-CCSD(T) interaction energies with improving basis sets for C3A and C3GC is shown on panel a) of Fig. S4 of the main text. The large BSSE obtained with the aug-cc-pVTZ, and to some extent also with the aug-cc-pVQZ basis set is apparent for both complexes. Such large BSSE also affects the extrapolation, the CBS(T,Q) results clearly overshoot the basis set limit due to the underestimation of the aug-cc-pVTZ result. The BSSE is significantly reduced by the CP correction. All CP corrected results (solid symbols) closely agree already at the aug-cc-pVTZ level. Most importantly, the CBS(Q,5) entries of both the CP corrected and uncorrected series match each other within a few tenth of a kcal mol⁻¹, providing strong indication of basis set saturation. Upon inspection of the CP corrected and uncorrected interaction energies of Table SII, this statement can be extended for the remaining six complexes as well.

The left and right panels of Fig. S6 collect CP uncorrected and corrected LNO-CCSD(T) interaction energies for the coronene dimer. The overbinding of the aug-cc-pVTZ and aug-cc-pVQZ results caused by the BSSE is again significant, close to 50 and 20%, respectively. With the exception of the overshooting CBS(T,Q) extrapolation, the aug-cc-pVXZ energies, with $X=T$, Q , and 5 , as well as the CBS(Q,5) extrapolation form a highly convincing, converging series of results both with and without CP correction. The CP corrected and uncorrected CBS results approach the region of convergence from the opposite directions, hence their average, i.e., the half CP corrected results appear to be the best estimate at

the CBS(Q,5) level. Concerning CBS(T,Q), the fully CP corrected results are found more reliable due to the excessive BSSE obtained with aug-cc-pVTZ.

Although we find the level of convergence regarding the basis set satisfactory, we invested additional efforts to perform LNO-CCSD(T)/aug-cc-pV6Z computations for the GGG complex. The CP corrected CBS(Q,5) and CBS(5,6) results at the very Tight LNO-CCSD(T) level agree up to 0.1 kcal mol⁻¹, which is within the local uncertainty.

Finally, we assess the accuracy of the composite BSI correction approach employed for C3A, C3GC, and C₆₀@[6]CPPA. Due to the prohibitive computational costs, the most accurate interaction energies presented here for these three systems are obtained by adding a $\Delta_{\text{BSI}} = E_{\text{Normal}}^{\text{LNO-CCSD(T)}}[\text{CBS(Q, 5)}] - E_{\text{Normal}}^{\text{LNO-CCSD(T)}}[\text{aug-cc-pVTZ}]$ BSI correction to the $E_{\text{Tight-very Tight}}^{\text{LNO-CCSD(T)}}[\text{aug-cc-pVTZ}]$ interaction energies. This formula exploits the similarity of the local approximation convergence curves obtained with different basis sets and it is numerically identical to $E_{\text{Tight-very Tight}}^{\text{LNO-CCSD(T)}}[\text{CBS(Q,5)}]$ if the local convergence patterns are exactly parallel. To assess the quality of Δ_{BSI} , we compared Δ_{BSI} to the analogous $\Delta_{\text{BSI}}^{\text{very Tight}} = E_{\text{very Tight}}^{\text{LNO-CCSD(T)}}[\text{CBS(Q, 5)}] - E_{\text{very Tight}}^{\text{LNO-CCSD(T)}}[\text{aug-cc-pVTZ}]$ wherever it is available. For the system most similar with the above three, that is, for C2C2PD, the $|\Delta_{\text{BSI}}^{\text{very Tight}} - \Delta_{\text{BSI}}|$ value is about 0.12 kcal mol⁻¹. To account for the potentially size-extensive nature of this unparallelity error, the final Δ_{BSI} error estimates of Table SII were obtained by scaling the 0.12 kcal mol⁻¹ with the ratio of the interaction energies of the given complex and C2C2PD. The ‘‘Total error bar’’ values of Table SII also include this third, Δ_{BSI} related uncertainty estimate for these three complexes.

Even more details can be learned observing the convergence of the total HF and the LNO-CCSD(T) correlation energies separately for the complexes and monomers (see Sect. S1 C). The HF total energies are converged to six significant digits at the CBS(Q,5) level, which translates into a highly convincing convergence level of 0.01 kcal mol⁻¹ regarding the HF part of the interaction energies. In other words, that BSI error estimates collected in Table SII have negligible HF and sizable correlation contribution. Furthermore, the CP corrected interaction energies are converged up to this 0.01 kcal mol⁻¹ level already with the smallest, aug-cc-pVTZ basis set. As expected, the CCSD(T) correlation energies tend significantly more slowly to the CBS limit with the cardinal number, but the agreement of the CBS(T,Q) and CBS(Q,5) values up to 4 significant digits is again highly satisfactory. This shows that the BSI error estimates being below 0.36 kcal mol⁻¹, just as the LNO error estimates, are

consistent with the absolute energies and do not benefit from sizable error compensation. Additionally, the computation of the interaction energies is warranted according to the supermolecular approach [see Eq. (1) of the main text], because total energies are converged to the necessary number of significant digits.

C. LNO-CCSD(T) energies plotted on Figs. S4. and S6

In Tables SIII–SV, we collect the absolute HF, the LNO-CCSD(T) correlation, and the corresponding interaction energies using all possible combinations of settings (*Normal* to *very Tight*, aug-cc-pVTZ to aug-cc-pV5Z, corresponding extrapolated energies, and various use of CP corrections) to document the numerical data plotted in Fig. S4 and S6. Additional analysis is provided in Sects. S1 A and S1 B.

TABLE SIII. HF energies and LNO-CCSD(T) correlation energies [in a.u.], and corresponding interaction energies [ΔE in kcal mol⁻¹] obtained for the C3GC dimer with all employed basis sets and LNO threshold combinations, including CBS and LNO extrapolations as well as full (CP) and half CP (half CP) corrected results.^a

	C3GC	circ.	GC	circ. CP	GC CP	ΔE	ΔE CP	ΔE half CP
aug-cc-pVTZ								
HF	-2988.683486	-2056.327131	-932.381768	-2056.328307	-932.383046	15.95	17.49	16.72
Normal	-12.6945	-8.8704	-3.7261	-8.8783	-3.7319	-45.57	-35.46	-40.52
Tight	-12.6941	-8.8746	-3.7284	-8.8824	-3.7341	-41.15	-31.19	-36.17
very Tight	-12.6955	-8.8771	-3.7294	-8.8848	-3.7352	-39.84	-29.90	-34.87
Normal-Tight	-12.6938	-8.8768	-3.7296	-8.8844	-3.7353	-38.93	-29.05	-33.99
Tight-very Tight	-12.6962	-8.8784	-3.7299	-8.8860	-3.7357	-39.19	-29.25	-34.22
aug-cc-pVQZ								
HF	-2988.845437	-2056.435660	-932.437072	-2056.435922	-932.437370	17.13	17.48	17.30
Normal	-13.2457	-9.2508	-3.9073	-9.2529	-3.9092	-37.84	-34.95	-36.40
Tight	-13.2452	-9.2551	-3.9096	-9.2570	-3.9115	-33.42	-30.67	-32.05
very Tight	-13.2467	-9.2576	-3.9106	-9.2595	-3.9125	-32.11	-29.38	-30.75
Normal-Tight	-13.2450	-9.2572	-3.9108	-9.2591	-3.9126	-31.20	-28.54	-29.87
Tight-very Tight	-13.2474	-9.2588	-3.9111	-9.2607	-3.9130	-31.46	-28.74	-30.10
aug-cc-pV5Z								
HF	-2988.878943	-2056.457991	-932.448732	-2056.458027	-932.448766	17.43	17.48	17.45
Normal	-13.4437	-9.3858	-3.9722	-9.3874	-3.9728	-36.35	-34.95	-35.65
Tight	-13.4432	-9.3901	-3.9745	-9.3914	-3.9751	-31.92	-30.67	-31.30
very Tight	-13.4446	-9.3926	-3.9755	-9.3939	-3.9761	-30.62	-29.38	-30.00
Normal-Tight	-13.4430	-9.3922	-3.9757	-9.3935	-3.9762	-29.71	-28.54	-29.12
Tight-very Tight	-13.4453	-9.3938	-3.9760	-9.3951	-3.9766	-29.97	-28.74	-29.35
CBS(T,Q)								
HF	-2988.889784	-2056.465378	-932.452216	-2056.465391	-932.452245	17.45	17.48	17.46
Normal	-13.6479	-9.5285	-4.0395	-9.5263	-4.0387	-32.74	-34.57	-33.66
Tight	-13.6475	-9.5327	-4.0418	-9.5304	-4.0409	-28.31	-30.30	-29.31
very Tight	-13.6489	-9.5352	-4.0428	-9.5329	-4.0420	-27.01	-29.01	-28.01
Normal-Tight	-13.6472	-9.5349	-4.0430	-9.5325	-4.0420	-26.10	-28.16	-27.13
Tight-very Tight	-13.6496	-9.5365	-4.0433	-9.5341	-4.0425	-26.36	-28.36	-27.36
CBS(Q,5)								
HF	-2988.884505	-2056.461698	-932.450668	-2056.461696	-932.450658	17.48	17.48	17.48
Normal	-13.6514	-9.5274	-4.0403	-9.5284	-4.0395	-35.05	-34.94	-35.00
Tight	-13.6509	-9.5317	-4.0426	-9.5325	-4.0417	-30.63	-30.67	-30.65
very Tight	-13.6524	-9.5342	-4.0436	-9.5349	-4.0428	-29.32	-29.38	-29.35
Normal-Tight	-13.6507	-9.5338	-4.0438	-9.5345	-4.0429	-28.42	-28.53	-28.47
Tight-very Tight	-13.6531	-9.5354	-4.0441	-9.5361	-4.0433	-28.67	-28.73	-28.70

^a Tight and very Tight results obtained with aug-cc-pVQZ and aug-cc-pV5Z, as well as any derivatives thereof employ the additive BSI correction according to the Methods and S1B Sections.

TABLE SIV. HF and LNO-CCSD(T) energies for systems of the C3A complex. See caption of SIII for more details.

	C3A	circ.	adenine	circ. CP	adenine CP	ΔE	ΔE CP	ΔE half CP
aug-cc-pVTZ								
HF	-2520.996126	-2056.327134	-464.682371	-2056.327896	-464.683038	8.40	9.29	8.84
Normal	-10.8264	-8.8705	-1.9001	-8.8753	-1.9033	-26.65	-20.77	-23.71
Tight	-10.8272	-8.8746	-1.9008	-8.8792	-1.9038	-24.12	-18.40	-21.26
very Tight	-10.8285	-8.8770	-1.9009	-8.8818	-1.9040	-23.32	-17.52	-20.42
Normal-Tight	-10.8276	-8.8767	-1.9011	-8.8812	-1.9041	-22.86	-17.22	-20.04
Tight-very Tight	-10.8291	-8.8783	-1.9010	-8.8831	-1.9040	-22.92	-17.08	-20.00
aug-cc-pVQZ								
HF	-2521.130595	-2056.435693	-464.709364	-2056.435867	-464.709527	9.08	9.29	9.18
Normal	-11.2905	-9.2505	-1.9900	-9.2518	-1.9912	-22.27	-20.53	-21.40
Tight	-11.2912	-9.2546	-1.9907	-9.2558	-1.9917	-19.74	-18.16	-18.95
very Tight	-11.2925	-9.2571	-1.9908	-9.2584	-1.9918	-18.94	-17.27	-18.11
Normal-Tight	-11.2916	-9.2567	-1.9910	-9.2577	-1.9920	-18.48	-16.97	-17.73
Tight-very Tight	-11.2932	-9.2583	-1.9909	-9.2597	-1.9919	-18.54	-16.83	-17.69
aug-cc-pV5Z								
HF	-2521.158239	-2056.458030	-464.714962	-2056.458051	-464.714981	9.26	9.28	9.27
Normal	-11.4564	-9.3855	-2.0221	-9.3867	-2.0225	-21.34	-20.26	-20.80
Tight	-11.4571	-9.3897	-2.0227	-9.3907	-2.0231	-18.81	-17.89	-18.35
very Tight	-11.4584	-9.3921	-2.0229	-9.3933	-2.0232	-18.01	-17.01	-17.51
Normal-Tight	-11.4575	-9.3917	-2.0231	-9.3927	-2.0234	-17.54	-16.70	-17.12
Tight-very Tight	-11.4591	-9.3933	-2.0229	-9.3946	-2.0233	-17.61	-16.56	-17.09
CBS(T,Q)								
HF	-2521.167416	-2056.465420	-464.716755	-2056.465433	-464.716780	9.26	9.29	9.27
Normal	-11.6291	-9.5278	-2.0556	-9.5266	-2.0553	-19.38	-20.35	-19.87
Tight	-11.6299	-9.5320	-2.0563	-9.5305	-2.0559	-16.86	-17.98	-17.42
very Tight	-11.6312	-9.5344	-2.0564	-9.5331	-2.0560	-16.06	-17.09	-16.57
Normal-Tight	-11.6303	-9.5340	-2.0566	-9.5325	-2.0562	-15.59	-16.79	-16.19
Tight-very Tight	-11.6318	-9.5356	-2.0565	-9.5344	-2.0560	-15.66	-16.65	-16.15
CBS(Q,5)								
HF	-2521.162828	-2056.461737	-464.715891	-2056.461734	-464.715887	9.29	9.28	9.28
Normal	-11.6304	-9.5272	-2.0557	-9.5283	-2.0555	-20.52	-19.97	-20.25
Tight	-11.6312	-9.5313	-2.0564	-9.5323	-2.0561	-17.99	-17.60	-17.80
very Tight	-11.6324	-9.5338	-2.0565	-9.5349	-2.0562	-17.19	-16.72	-16.95
Normal-Tight	-11.6315	-9.5334	-2.0567	-9.5342	-2.0563	-16.73	-16.42	-16.57
Tight-very Tight	-11.6331	-9.5350	-2.0566	-9.5362	-2.0562	-16.79	-16.28	-16.53

TABLE SV. HF and LNO-CCSD(T) energies for systems of the C2C2PD complex. See caption of SIII for more details.^a

	C2C2PD	coronene	coronene CP	ΔE	ΔE CP	ΔE half CP
aug-cc-pVTZ						
HF	-1832.429002	-916.226325	-916.227229	14.84	15.97	15.41
Normal	-8.0606	-3.9915	-3.9968	-33.84	-26.01	-29.92
Tight	-8.0585	-3.9929	-3.9982	-30.76	-22.93	-26.84
very Tight	-8.0574	-3.9932	-3.9985	-29.68	-22.01	-25.84
Normal–Tight	-8.0574	-3.9936	-3.9989	-29.22	-21.39	-25.30
Tight–very Tight	-8.0569	-3.9934	-3.9986	-29.14	-21.55	-25.34
aug-cc-pVQZ						
HF	-1832.526572	-916.275811	-916.276010	15.72	15.97	15.84
Normal	-8.3972	-4.1641	-4.1655	-27.58	-25.62	-26.60
Tight	-8.3898	-4.1628	-4.1641	-24.57	-22.66	-23.62
very Tight	-8.3866	-4.1621	-4.1635	-23.49	-21.43	-22.46
Normal–Tight	-8.3861	-4.1622	-4.1635	-23.07	-21.19	-22.13
Tight–very Tight	-8.3850	-4.1617	-4.1632	-22.94	-20.82	-21.88
aug-cc-pV5Z						
HF	-1832.546868	-916.286130	-916.286155	15.93	15.97	15.95
Normal	-8.5176	-4.2252	-4.2258	-26.24	-25.44	-25.84
Tight	-8.5008	-4.2194	-4.2199	-22.98	-22.33	-22.66
very Tight	-8.4937	-4.2166	-4.2171	-22.05	-21.33	-21.69
Normal–Tight	-8.4924	-4.2165	-4.2169	-21.35	-20.78	-21.07
Tight–very Tight	-8.4901	-4.2152	-4.2158	-21.59	-20.83	-21.21
CBS(T,Q)						
HF	-1832.553290	-916.289361	-916.289368	15.96	15.97	15.96
Normal	-8.6429	-4.2901	-4.2886	-23.42	-25.34	-24.38
Tight	-8.6316	-4.2868	-4.2852	-20.46	-22.47	-21.46
very Tight	-8.6268	-4.2852	-4.2839	-19.37	-21.01	-20.19
Normal–Tight	-8.6260	-4.2852	-4.2835	-18.98	-21.03	-20.00
Tight–very Tight	-8.6243	-4.2845	-4.2833	-18.83	-20.28	-19.55
CBS(Q,5)						
HF	-1832.550237	-916.287842	-916.287839	15.97	15.96	15.97
Normal	-8.6439	-4.2893	-4.2891	-25.02	-25.25	-25.13
Tight	-8.6172	-4.2788	-4.2784	-21.50	-21.98	-21.74
very Tight	-8.6061	-4.2738	-4.2734	-20.74	-21.22	-20.98
Normal–Tight	-8.6039	-4.2735	-4.2730	-19.74	-20.35	-20.05
Tight–very Tight	-8.6005	-4.2713	-4.2709	-20.36	-20.84	-20.60

^a Tight and very Tight results obtained with aug-cc-pVQZ and aug-cc-pV5Z are also directly evaluated without relying on the additive BSI correction according to the Methods and S1 B Sections.

D. Core and higher-order correlation on top of CCSD(T)

Core correlation effects are evaluated using the highly-optimized density-fitting (DF) MP2 implementation of the MRCC package [52] using large basis sets. In that way, the magnitude of the frozen core approximation can be determined independently from the local and BSI errors. The augmented weighted core-valence basis sets [82], aug-cc-pwCVXZ with $X=T$ and Q, were employed in combination with CP corrections. The core correlated DF-MP2 interaction energies of the C2C2PD complex, both with aug-cc-pwCVTZ and with aug-cc-pwCVQZ, as well as with CBS(T,Q), are consistently stronger by $0.22 \text{ kcal mol}^{-1}$ (4.6 cal mol^{-1} per C atom) than those obtained using the frozen core approach and otherwise identical settings.

The missing higher-order electron correlation on top of the CCSD(T) treatment was estimated using the CCSDT(Q) scheme, which includes infinite-order three-electron and the perturbative four-electron contributions [65]. As the conventional ninth power-scaling CCSDT(Q) calculations are many-orders of magnitude more expensive than CCSD(T), we relied on the analogous LNO approximations implemented also for CCSDT(Q) [13, 79] in the MRCC package [52]. Considering that large basis set CCSDT(Q) computations are only feasible for systems with only a few atoms, highly-converged LNO-CCSDT(Q) computations are still well beyond the current capabilities even for the smallest GGG complex. With relying on looser LNO truncations and the moderate basis set of 6-31G**(0.25,0.15) [23], we were able to perform by far the largest LNO-CCSDT(Q) calculation ever presented for the GGG complex. The cumulative local and BSI error of the LNO-CCSDT(Q) interaction energies are estimated to be about 38% at the corresponding LNO-CCSD(T)/6-31G**(0.25,0.15) level. Up to this uncertainty, the CCSDT contribution on top of CCSD(T) is found to be $-0.013 \text{ kcal mol}^{-1}$, while the (Q) correction on top of CCSDT is about $-0.021 \text{ kcal mol}^{-1}$. Clearly, both corrections are negligibly small compared to the deviation of CCSD(T) and FN-DMC. As the even higher-order CC terms are expected to be even smaller, it is unlikely that higher-order electron correlation effects missing from CCSD(T) could completely explain the disagreement of CCSD(T) and FN-DMC.

The weakly-correlated character of the studied system is also verified via the T1 [83] diagnostics. The T1 measures obtained for the most complicated C3GC and C₆₀@[6]CPPA complexes are found to be at most 0.016 and 0.014, respectively. Considering that the T1

measure grows with the number of basis functions and that smaller than 0.02 T1 values are considered weakly-correlated already for very small systems [83], there appears to be no indication of even moderate static correlation. Moreover, neither the HF nor the CCSD iterations indicated any problems emerging usually for strongly correlated systems. The size of the singles and doubles amplitudes were also monitored in all domain CCSD computations indicating the validity of the single-reference approach, while it is convincing that the LNO approximations were found to operate excellently also for moderately statically correlated species [84]. The magnitude of the (T) correction compared to the full CCSD(T) interaction energy is also an informative measure of the static or dynamic nature of the correlation. This ratio is consistently around 18-20% for all 8 complexes, which is well within the range observed for smaller and simpler systems, e.g., in the well-known S66 test set (cca. 13–24%) [85].

S2. DETAILS OF QUANTUM MONTE CARLO CALCULATIONS

The FN-DMC calculations mostly used 10 nodes with 28 cores each, and 14,000 walkers distributed across the cores (*i.e.* 50 walkers per core). We used 20 nodes for the C₆₀@[6]CPPA complex and 28,000 walkers to reduce the stochastic error in a shorter time. Here we give further details on (i) the optimization of the Jastrow factor for the reported complexes, (ii) time-step and node-structure tests for the coronene dimer and (iii) results of additional FN-DMC simulations of C₆₀@[6]CPPA. In addition, we report the total energies for C3A and C3GC complexes here in Table SVI.

A. Variational Monte Carlo Optimization of the Jastrow Factor

Variational Monte Carlo (VMC) obeys the variational principle, allowing the initial Slater-Jastrow wavefunction to be optimized iteratively towards a lower energy. Importantly, the zero-variance principle ensures that variance of the energy tends to zero as the exact energy of the system is approached. This is used in the varmin and varmin–linjas optimization algorithms in CASINO [73] to optimize the variable parameters of the Jastrow factor. The Jastrow factor is composed of explicit distance-dependent polynomial functions for inter-particle interactions, such as electron-electron (u), electron-nucleus (χ), and

TABLE SVI. The total energy in Ha for each complex and its monomers are given here with stochastic errors from FN-DMC calculations alongside description of the DFT orbitals and plane-wave cut-offs (in Ry) and FN-DMC time step (in a.u.) and algorithm (*i.e.* standard locality approximation (LA) or determinant localization approximation (DLA)). Resulting interaction energy (IE) is reported lastly.

FN-DMC setup	C3GC	circ.	GC	IE (kcal mol ⁻¹)
LDA orb/500Ry, 0.03 time-step/LA	-485.928809 ± 0.000934	-317.320337 ± 0.000485	-168.569987 ± 0.000209	-24.2 ± 0.7
PBE0 orb/400Ry, 0.03 time-step/LA	-485.939114 ± 0.001047	-317.326450 ± 0.000731	-168.575218 ± 0.000148	-23.5 ± 0.8
PBE0 orb/400Ry, 0.01 time-step/LA	-485.933462 ± 0.000881	-317.325540 ± 0.000579	-168.570123 ± 0.000603	-23.8 ± 0.8
FN-DMC setup	C3A	circ.	adenine	IE (kcal mol ⁻¹)
LDA orb/500Ry, 0.03 time-step/LA	-398.351177 ± 0.000648	-317.320307 ± 0.000492	-81.006922 ± 0.000162	-15.0 ± 0.5
LDA orb/500Ry, 0.01 time-step/LA	-398.351280 ± 0.000966	-317.321748 ± 0.000886	-81.006670 ± 0.000196	-14.3 ± 0.8
LDA orb/500Ry, 0.01 time-step/DLA	-398.438355 ± 0.000546	-317.393190 ± 0.000585	-81.022893 ± 0.000228	-14.0 ± 0.5

electron-electron-nucleus (f), and is also system-dependent. For all complexes, we performed a term-by-term optimization using 24 parameters for u , 12-14 parameters per element for χ , and 8 parameters per element for f . The resulting VMC energy and variance for the complexes is given in Table SVII.

TABLE SVII. The variance (σ^2) and VMC energy (E_{VMC}) in atomic units for each complex, as a result of optimizing the trial wavefunction. The uncertainty is indicated in parentheses.

Complex	σ^2	E_{VMC}
CBH	4.07(5)	-249.26(1)
C2C2PD	4.76(6)	-285.769(8)
GGG	5.18(3)	-290.195(5)
GCGC	5.71(3)	-336.296(1)
PHE	6.03(4)	-367.239(8)
C3A	6.38(4)	-397.085(6)
C3GC	7.82(5)	-484.474(7)
C ₆₀ @[6]CPPA	10.54(5)	-624.140(6)

B. Time-Step and Node-Structure Dependence of the Coronene Dimer

It can be seen from Fig. S7 that the FN-DMC interaction energy of C2C2PD is converged within the stochastic error bar (corresponding to 1 standard deviation) with respect to the time-step in FN-DMC (from 0.003 to 0.03 a.u.). In addition, we computed PBE0 and PBE initial determinants (orbitals) from PWSCF, in order to assess the FN-DMC dependence of the interaction energy on the nodal-structure. Fig. S7 shows that the FN-DMC interaction energy is the same within the stochastic error bars of ~ 0.5 kcal mol⁻¹ across the three nodal-structures.

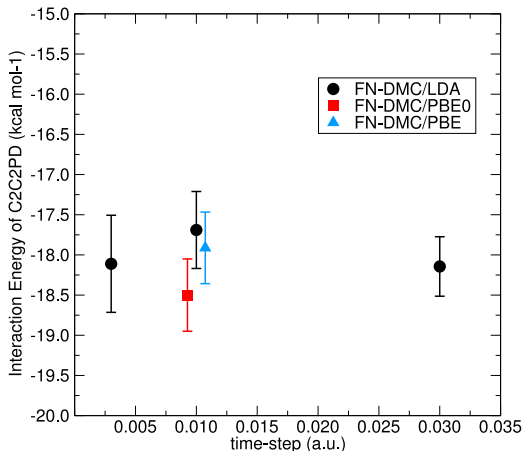


FIG. S7. FN-DMC interaction energy of C2C2PD (coronene dimer) with 0.003, 0.01 and 0.03 a.u. time-steps. Different nodal-structures from LDA (black circle), PBE (blue triangle), and PBE0 (red square) initial orbitals are reported using 0.01 a.u. time-step; these are slightly offset along the x-axis for clarity.

C. The GGG Trimer and Coronene Dimer with the Determinant Localization Approximation

Using non-local pseudopotentials in FN-DMC requires an approximation for the evaluation of the local energy – not to be confused with the type of local approximations, such as LNO, made in local CCSD(T) methods. The recent determinant localization approximation (DLA) introduced by Zen *et al.* [54] has some advantages over the pre-existing standard algorithms: the locality approximation [74] (LA) and T-move scheme [75]). The DLA FN-DMC

energies are less sensitive to the Jastrow factor that is used in combination with pseudopotentials at larger time-steps. This enables better overall convergence with the time-step in FN-DMC and the DLA method is also more numerically stable than LA. We tested the use of the DLA method for the GGG trimer and the coronene dimer and present the results in Table SVIII. The interaction energies of the GGG and C2C2PD complexes remain in

TABLE SVIII. Comparison of the standard LA to the DLA method in the GGG and C2C2PD complexes.

Complex	Approximation	Time-step	IE (kcal mol ⁻¹)
GGG	standard LA	0.03	1.5 ± 0.3
GGG	DLA	0.03	1.4 ± 0.2
C2C2PD	standard LA	0.03	-18.1 ± 0.4
C2C2PD	DLA	0.01	-17.4 ± 0.5

agreement, within the one-standard deviation stochastic errors, between the DLA and the standard LA algorithms. The results support that the FN-DMC results are converged with respect to the time-steps and employed Jastrow factors.

D. FN-DMC with T-move on the C₆₀@[6]CPPA Complex

The C₆₀@[6]CPPA complex proved to be more challenging to compute with FN-DMC, due to numerical instabilities when using the locality approximation. This was alleviated by the use of the DLA method, and separately using the T-move approximation in place of the locality approximation. The T-move scheme reinstates variational form of the energy, but the energies with this approximation are more time-step dependent, as can be seen in Fig. S8. Linear extrapolations to 'zero' time-step limit yield -31.14 ± 2.57 kcal mol⁻¹ using LDA orbitals and -29.16 ± 2.33 kcal mol⁻¹ using PBE0 orbitals. Moreover, we show the DLA obtained FN-DMC interaction energy at 0.03 and 0.01 a.u. time-steps. In this way, the independence of the interaction energy on the nodal structure and the FN-DMC algorithm is established.

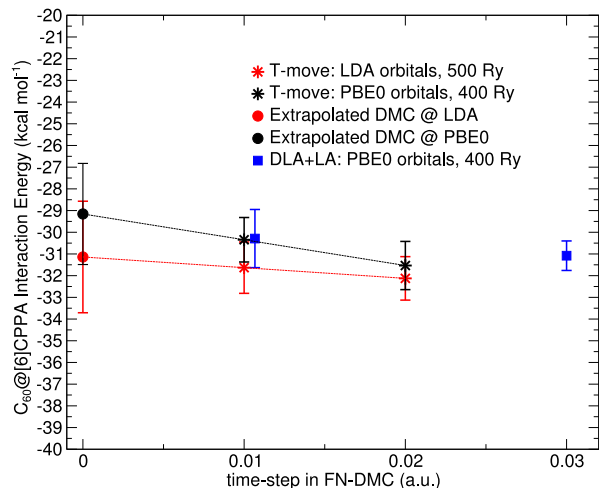


FIG. S8. FN-DMC interaction energy of $C_{60}@[6]CPPA$ complex using two algorithms. T-move interaction energies at 0.01 and 0.02 a.u. time-steps are shown for LDA (black stars) and PBE0 orbitals (red stars). The linear extrapolation to zero time-step for each set is indicated by the dashed lines, with the result in circles. The error on the zero time-step FN-DMC interaction energies are propagated according to the extrapolation. For comparison, the DLA method is shown (with the locality approximation) in blue squares. The DLA FN-DMC interaction energy at 0.01 a.u. is slightly offset along the x-axis for clarity.

S3. COMPUTATIONAL REQUIREMENTS OF LNO-CCSD(T) AND FN-DMC

CPU core time and minimal memory requirements are collected in Table S2D for representative examples: the CBH and C3GC complexes. The very Tight LNO-CCSD(T)/aug-cc-pVTZ computation for C3GC was found to be the upper limit for the CPU time requirement among all LNO-CCSD(T) computations. Compared to that it is interesting to note the case of CBH, which contains even more atoms and almost as much AOs as C3GC. However, due to the relatively low complexity of the wavefunction of CBH, its CPU time demand is found to be up to 100 times smaller than that of C3GC when using the same settings. Unfortunately, the computations were scattered on multiple clusters and CPU types preventing the straightforward comparison of runtimes with various settings. For that reason CPU core times and the corresponding CPU types are reported. With that in mind, we find similar trends as in our previous report [14]. For instance, the memory requirement of LNO-CCSD(T) is exceptionally small compared to alternative CCSD(T) implementations,

which was essential for the C3A, C3GC, and C₆₀@[6]CPPA computations. Moreover, about 3-5 times more operations were performed when using one step tighter LNO settings, just as in our previous computations [14], which trend is highly useful to estimate the feasibility of analogous computations. It is also important to note that the CPU and memory requirement grow much more slowly with the basis set size than with conventional CCSD(T), where the operation count and data storage increase by about a factor of 10 with one step in the cardinal number hierarchy (e.g., from aug-cc-pVTZ to aug-cc-pVQZ).

Compared to LNO-CCSD(T), the FN-DMC runtimes depend less on the chemical composition and can be estimated more accurately based on the number of computed particles. The notably small memory requirement and the ease of efficient parallelization are also apparent benefits of the FN-DMC method. Moreover, the computational cost of FN-DMC does not change as steeply with various input nodal structures and time-steps allowing for the estimation of these effects using manageable additional computational time.

TABLE SIX. CPU core time (i.e., [number of nodes]*[core per node]*[wall time in years]) and minimum memory [in GB] requirement of the LNO-CCSD(T) and FN-DMC calculations for the CBH and C3GC complexes with all settings.

Complex:	CBH		C3GC	
No. of atoms:	112		101	
	memory [GB]	time [core year]	memory [GB]	time [core year]
LNO-CCSD(T) AOs in aug-cc-pVTZ:	3404		4002	
Normal	3 [#]	0.02 ^a	70 [#]	0.4 ^a
Tight	7 [#]	0.08 ^a	73 [#]	3.6 ^{a,b,e,*}
very Tight	12 [#]	0.2 ^a	200	20 ^{c,g,*}
AOs in aug-cc-pVQZ:	6376		7128	
Normal	11 [#]	0.04 ^a	110 [#]	1.6 ^{a,*}
Tight	24 [#]	0.13 ^a	-	-
very Tight	29 [#]	0.4 ^d	-	-
AOs in aug-cc-pV5Z:	10652		11511	
Normal	32 [#]	0.1 ^e	63	2.7 ^{f,*}
Tight	50 [#]	0.3 ^h	-	-
very Tight	86 [#]	1.2 ^{f,*}	-	-
FN-DMC LA/0.03 a.u.	7 [†]	2.5 ^{c,e}	15 [†]	3.3 ^{c,e}

^a Intel Xeon E5-2670 v3 2.3 GHz ^b Intel Xeon E5-1650 v2 3.5 GHz ^c Intel Xeon Gold 6132 2.3 GHz ^d Intel Xeon E5-2680 v2 2.8 GHz ^e Intel Xeon E5-2680 v4 2.4 GHz ^f Intel Xeon E5-2680 v3 2.5 GHz ^g Intel Xeon Platinum 8180M 2.3 GHz ^h Intel Xeon Gold 6138 1.9 GHz * Estimated CPU time due to large number of restarts. # Fully integral-direct integral transformation, minimal memory algorithm would require about up to 3-4 times less memory. † Maximum shared memory used, mainly determined by size of wavefunction file.

S4. DETAILS OF DFT CALCULATIONS

The PBE0+MBD calculations were performed using FHI-aims v.190225 with all-electron numerical basis sets, with “tight” defaults and tier 2 basis functions for all elements. The total energy threshold for self-consistent convergence was set to 10^{-7} eV. Spin and relativistic effects have not been included. London dispersion energies from the D4 model are computed with the DFTD4 standalone program using the electronegativity equilibration charges (EEQ) and include a coupled-dipole based many-body dispersion correction (D4(EEQ)-MBD) [26]. The same geometries have been used as for the benchmark calculations for all structures.

S5. GEOMETRY OF THE L7 AND THE C₆₀@[6]CPPA COMPLEXES

The structures and fragment definitions in Ref. 23 were used for the L7 calculations. For C₆₀@[6]CPPA, a C₇₀@[6]CPPA geometry from Ref. 42 was modified, by replacing C₇₀ with C₆₀ and the complex was symmetrized to D_{3d} point group. The high-symmetry structure allows more efficient calculations with LNO-CCSD(T) with a speedup proportional to the rank of the point group [13, 79]. The stability of this complex was assessed by relaxing the geometry whilst retaining the symmetry group, at the DFT level (B97-3c exchange-correlation functional). The interaction strength increases by less than 0.1 kcal mol⁻¹ with respect to the unrelaxed structure. Relaxing the C₆₀ and [6]CPPA fragments reduces the interaction strength by 0.9 kcal mol⁻¹.

The C₆₀@[6]CPPA Cartesian coordinates used in LNO-CCSD(T) and FN-DMC calculations is given here.

```
C -0.72650728 -1.22225849 -3.24715547
C 0.72650728 -1.22225849 -3.24715547
C -1.42176054 -0.01804451 -3.24715547
C 1.42176054 -0.01804451 -3.24715547
C 2.59727407 0.14217202 -2.40825772
C 1.17551245 -2.32039134 -2.40825772
C 2.30045705 -2.16706760 -1.60544793
C 3.02696412 -0.90872044 -1.60544793
C -3.02696412 -0.90872044 -1.60544793
```

C -2.30045705 -2.16706760 -1.60544793
C -2.59727407 0.14217202 -2.40825772
C -1.17551245 -2.32039134 -2.40825772
C 0.00000000 -2.99907290 -1.88979043
C -2.30045914 -2.68553418 -0.24808191
C -1.17551125 -3.33502315 0.24808191
C 0.00000000 -3.49523729 -0.59081634
C -3.02696429 1.74761865 -0.59081634
C -3.47597040 0.64948897 0.24808191
C -2.59727332 1.49953645 -1.88979043
C -3.47597040 -0.64948897 -0.24808191
C -3.02696429 -1.74761865 0.59081634
C -3.02696412 0.90872044 1.60544793
C -2.59727407 -0.14217202 2.40825772
C -2.59727332 -1.49953645 1.88979043
C -0.72650707 3.07578804 -1.60544793
C -1.17551125 3.33502315 -0.24808191
C -1.42176162 2.17821932 -2.40825772
C -2.30045914 2.68553418 0.24808191
C -2.30045705 2.16706760 1.60544793
C -0.00000000 3.49523729 0.59081634
C -0.00000000 2.99907290 1.88979043
C -1.17551245 2.32039134 2.40825772
C 0.69525326 1.24030300 -3.24715547
C 1.42176162 2.17821932 -2.40825772
C -0.69525326 1.24030300 -3.24715547
C 0.72650707 3.07578804 -1.60544793
C 1.17551125 3.33502315 -0.24808191
C 2.59727332 1.49953645 -1.88979043
C 3.02696429 1.74761865 -0.59081634
C 2.30045914 2.68553418 0.24808191
C 0.72650728 1.22225849 3.24715547

C 1.17551245 2.32039134 2.40825772
C 2.30045705 2.16706760 1.60544793
C 1.42176054 0.01804451 3.24715547
C -0.69525326 -1.24030300 3.24715547
C -1.42176054 0.01804451 3.24715547
C -0.72650728 1.22225849 3.24715547
C 0.69525326 -1.24030300 3.24715547
C 0.72650707 -3.07578804 1.60544793
C -0.72650707 -3.07578804 1.60544793
C -1.42176162 -2.17821932 2.40825772
C 1.42176162 -2.17821932 2.40825772
C 3.02696429 -1.74761865 0.59081634
C 2.30045914 -2.68553418 -0.24808191
C 1.17551125 -3.33502315 0.24808191
C 2.59727332 -1.49953645 1.88979043
C 3.02696412 0.90872044 1.60544793
C 3.47597040 0.64948897 0.24808191
C 3.47597040 -0.64948897 -0.24808191
C 2.59727407 -0.14217202 2.40825772
C -4.43498968 4.84818396 -0.00326334
C -5.43089278 3.84285784 -0.00366147
C -3.85193459 5.28074380 -1.21899357
C -3.85171966 5.27950986 1.21280412
C -2.64632983 5.97544200 -1.21280412
C -2.64729099 5.97624511 1.21899357
C -1.98115563 6.26490571 0.00326334
C -6.04345890 2.78186219 -0.00366147
H -4.31742848 4.99255327 -2.16174586
H -4.31701338 4.99032575 2.15534928
H -2.16324219 6.23380613 -2.15534928
H -2.16496372 6.23527938 2.16174586
C 1.98115563 6.26490571 0.00326334

C 0.61256612 6.62472003 0.00366147
C 2.64632983 5.97544200 -1.21280412
C 2.64729099 5.97624511 1.21899357
C 3.85193459 5.28074380 -1.21899357
C 3.85171966 5.27950986 1.21280412
C 4.43498968 4.84818396 -0.00326334
C -0.61256612 6.62472003 0.00366147
H 2.16324219 6.23380613 -2.15534928
H 2.16496372 6.23527938 2.16174586
H 4.31742848 4.99255327 -2.16174586
H 4.31701338 4.99032575 2.15534928
C 6.41614531 1.41672175 -0.00326334
C 6.04345890 2.78186219 -0.00366147
C 6.49922558 0.69550131 -1.21899357
C 6.49804949 0.69593214 1.21280412
C 6.49804949 -0.69593214 -1.21280412
C 6.49922558 -0.69550131 1.21899357
C 6.41614531 -1.41672175 0.00326334
C 5.43089278 3.84285784 -0.00366147
H 6.48239220 1.24272611 -2.16174586
H 6.48025557 1.24348038 2.15534928
H 6.48025557 -1.24348038 -2.15534928
H 6.48239220 -1.24272611 2.16174586
C 4.43498968 -4.84818396 0.00326334
C 5.43089278 -3.84285784 0.00366147
C 3.85171966 -5.27950986 -1.21280412
C 3.85193459 -5.28074380 1.21899357
C 2.64729099 -5.97624511 -1.21899357
C 2.64632983 -5.97544200 1.21280412
C 1.98115563 -6.26490571 -0.00326334
C 6.04345890 -2.78186219 0.00366147
H 4.31701338 -4.99032575 -2.15534928

H 4.31742848 -4.99255327 2.16174586
H 2.16496372 -6.23527938 -2.16174586
H 2.16324219 -6.23380613 2.15534928
C -1.98115563 -6.26490571 -0.00326334
C -0.61256612 -6.62472003 -0.00366147
C -2.64729099 -5.97624511 -1.21899357
C -2.64632983 -5.97544200 1.21280412
C -3.85171966 -5.27950986 -1.21280412
C -3.85193459 -5.28074380 1.21899357
C -4.43498968 -4.84818396 0.00326334
C 0.61256612 -6.62472003 -0.00366147
H -2.16496372 -6.23527938 -2.16174586
H -2.16324219 -6.23380613 2.15534928
H -4.31701338 -4.99032575 -2.15534928
H -4.31742848 -4.99255327 2.16174586
C -6.41614531 -1.41672175 0.00326334
C -6.04345890 -2.78186219 0.00366147
C -6.49804949 -0.69593214 -1.21280412
C -6.49922558 -0.69550131 1.21899357
C -6.49922558 0.69550131 -1.21899357
C -6.49804949 0.69593214 1.21280412
C -6.41614531 1.41672175 -0.00326334
C -5.43089278 -3.84285784 0.00366147
H -6.48025557 -1.24348038 -2.15534928
H -6.48239220 -1.24272611 2.16174586
H -6.48239220 1.24272611 -2.16174586
H -6.48025557 1.24348038 2.15534928

[1] E. A. Carter, Challenges in Modeling Materials Properties Without Experimental Input, *Science* **321**, 800 (2008).

- [2] M. Dubecký, P. Jurečka, R. Derian, P. Hobza, M. Otyepka, and L. Mitáš, Quantum Monte Carlo methods describe noncovalent interactions with subchemical accuracy, *J. Chem. Theor. Comput.* **9**, 4287 (2013).
- [3] J. Yang, W. Hu, D. Usvyat, D. Matthews, M. Schütz, and G. K.-L. Chan, Ab initio determination of the crystalline benzene lattice energy to sub-kilojoule/mole accuracy, *Science* **345**, 640 (2014).
- [4] A. M. Reilly, R. I. Cooper, C. S. Adjiman, S. Bhattacharya, A. D. Boese, J. G. Brandenburg, P. J. Bygrave, R. Bylisma, J. E. Campbell, R. Car, *et al.*, Report on the sixth blind test of organic crystal structure prediction methods, *Acta Crystallographica Section B Structural Science, Crystal Engineering and Materials* **72**, 439 (2016).
- [5] K. Müller-Dethlefs and P. Hobza, Noncovalent Interactions: A Challenge for Experiment and Theory, *Chem. Rev.* **100**, 143 (2000).
- [6] Y. Wang, Y. Liu, S. Song, Z. Yang, X. Qi, K. Wang, Y. Liu, Q. Zhang, and Y. Tian, Accelerating the discovery of insensitive high-energy-density materials by a materials genome approach, *Nat. Commun.* **9**, 2444 (2018).
- [7] Y. Lee, S. D. Barthel, P. Dłotko, S. M. Moosavi, K. Hess, and B. Smit, High-Throughput Screening Approach for Nanoporous Materials Genome Using Topological Data Analysis: Application to Zeolites, *J. Chem. Theor. Comput.* **14**, 4427 (2018).
- [8] D. Ongari, A. V. Yakutovich, L. Talirz, and B. Smit, Building a Consistent and Reproducible Database for Adsorption Evaluation in CovalentOrganic Frameworks, *ACS Central Science* **5**, 1663 (2019).
- [9] Y. S. Al-Hamdani and A. Tkatchenko, Understanding non-covalent interactions in larger molecular complexes from first principles, *J. Chem. Phys.* **150**, 010901 (2019).
- [10] K. Liao, X.-Z. Li, A. Alavi, and A. Grüneis, A comparative study using state-of-the-art electronic structure theories on solid hydrogen phases under high pressures, *npj Computational Materials* **5**, 110 (2019).
- [11] J. G. Brandenburg, A. Zen, M. Fitzner, B. Ramberger, G. Kresse, T. Tsatsoulis, A. Grüneis, A. Michaelides, and D. Alfè, Physisorption of water on graphene: Subchemical accuracy from many-body electronic structure methods, *J. Phys. Chem. Lett.* **10**, 358 (2019).
- [12] K. Raghavachari, G. W. Trucks, J. A. Pople, and M. Head-Gordon, A fifth-order perturbation comparison of electron correlation theories, *Chem. Phys. Lett.* **157**, 479 (1989).

- [13] P. R. Nagy, G. Samu, and M. Kállay, Optimization of the linear-scaling local natural orbital CCSD(T) method: Improved algorithm and benchmark applications, *J. Chem. Theory Comput.* **14**, 4193 (2018).
- [14] P. R. Nagy and M. Kállay, Approaching the basis set limit of CCSD(T) energies for large molecules with local natural orbital coupled-cluster methods, *J. Chem. Theory Comput.* **15**, 5275 (2019).
- [15] I. Shavitt and R. Bartlett, *Many-Body Methods in Chemistry and Physics: MBPT and Coupled-Cluster Theory*, Cambridge Molecular Science (Cambridge University Press, 2009).
- [16] M. Dubecký, L. Mitas, and P. Jurečka, Noncovalent Interactions by Quantum Monte Carlo, *Chem. Rev.* **116**, 5188 (2016).
- [17] A. Zen, J. G. Brandenburg, J. Klimeš, A. Tkatchenko, D. Alfè, and A. Michaelides, Fast and accurate quantum Monte Carlo for molecular crystals, *Proc. Natl. Acad. Sci.* **115**, 1724 (2018).
- [18] Y. S. Al-Hamdani, D. Alfè, and A. Michaelides, How strongly do hydrogen and water molecules stick to carbon nanomaterials?, *J. Chem. Phys.* **146**, 094701 (2017).
- [19] A. Ambrosetti, N. Ferri, R. A. DiStasio Jr., and A. Tkatchenko, Wavelike charge density fluctuations and van der waals interactions at the nanoscale, *Science* **351**, 1171 (2016).
- [20] K. D. Jordan and A. Heßelmann, Comment on Physisorption of Water on Graphene: Subchemical Accuracy from Many-Body Electronic Structure Methods, *J. Phys. Chem. C* **123**, 10163 (2019).
- [21] G. R. Jenness, O. Karalti, and K. D. Jordan, Benchmark calculations of water-acene interaction energies: Extrapolation to the water-graphene limit and assessment of dispersion-corrected DFT methods, *Physical Chemistry Chemical Physics* **12**, 6375 (2010).
- [22] B. D. Nguyen, G. P. Chen, M. M. Agee, A. M. Burow, M. P. Tang, and F. Furche, Divergence of many-body perturbation theory for noncovalent interactions of large molecules, *J. Chem. Theory Comput.* **16**, 2258 (2020).
- [23] R. Sedlak, T. Janowski, M. Pitoňák, J. Řezáč, P. Pulay, and P. Hobza, Accuracy of quantum chemical methods for large noncovalent complexes, *J. Chem. Theory Comput.* **9**, 3364 (2013).
- [24] R. Antoine, P. Dugourd, D. Rayane, E. Benichou, M. Broyer, F. Chandezon, and C. Guet, Direct measurement of the electric polarizability of isolated C60 molecules, *J. Chem. Phys.* **110**, 9771 (1999).

- [25] M. Sadhukhan and A. Tkatchenko, Long-range repulsion between spatially confined van der waals dimers, *Phys. Rev. Lett.* **118**, 210402 (2017).
- [26] E. Caldeweyher, S. Ehlert, A. Hansen, H. Neugebauer, S. Spicher, C. Bannwarth, and S. Grimme, A generally applicable atomic-charge dependent london dispersion correction, *J. Chem. Phys.* **150**, 154122 (2019).
- [27] A. Ambrosetti, A. M. Reilly, R. A. DiStasio, Jr., and A. Tkatchenko, Long-range correlation energy calculated from coupled atomic response functions, *J. Chem. Phys.* **140**, 18A508 (2014).
- [28] J. Hermann, R. A. DiStasio, and A. Tkatchenko, First-Principles Models for van der Waals Interactions in Molecules and Materials: Concepts, Theory, and Applications, *Chem. Rev.* **117**, 4714 (2017).
- [29] S. Grimme, A. Hansen, J. G. Brandenburg, and C. Bannwarth, Dispersion-Corrected Mean-Field Electronic Structure Methods, *Chem. Rev.* **116**, 5105 (2016).
- [30] G. H. Booth, A. Grüneis, G. Kresse, and A. Alavi, Towards an exact description of electronic wavefunctions in real solids, *Nature* **493**, 365 (2013).
- [31] J. S. Kottmann and F. A. Bischoff, Coupled-Cluster in real space. 1. CC2 ground state energies using multiresolution analysis, *J. Chem. Theory Comput.* **13**, 5945 (2017).
- [32] C. Riplinger, B. Sandhoefer, A. Hansen, and F. Neese, Natural triple excitations in local coupled cluster calculations with pair natural orbitals, *J. Chem. Phys.* **139**, 134101 (2013).
- [33] Q. Ma and H.-J. Werner, Explicitly correlated local coupled-cluster methods using pair natural orbitals, *Wiley Interdiscip. Rev. Comput. Mol. Sci.* **8**, e1371 (2018).
- [34] G. Schmitz, C. Hattig, and D. P. Tew, Explicitly correlated PNO-MP2 and PNO-CCSD and their application to the S66 set and large molecular systems, *Phys. Chem. Chem. Phys.* **16**, 22167 (2014).
- [35] F. Pavošević, C. Peng, P. Pinski, C. Riplinger, F. Neese, and E. F. Valeev, Sparsemaps—a systematic infrastructure for reduced scaling electronic structure methods. v. linear scaling explicitly correlated coupled-cluster method with pair natural orbitals, *J. Chem. Phys.* **146**, 174108 (2017).
- [36] M. J. Deible, M. Kessler, K. E. Gasperich, and K. D. Jordan, Quantum Monte Carlo calculation of the binding energy of the beryllium dimer, *J. Chem. Phys.* **143**, 084116 (2015).
- [37] B. M. Flöser, Y. Guo, C. Riplinger, F. Tuzcek, and F. Neese, Detailed pair natural orbital-based coupled cluster studies of spin crossover energetics, *J. Chem. Theory Comput.* **16**, 2224

- (2020).
- [38] J. Řezáč, M. Dubecký, P. Jurečka, and P. Hobza, Extensions and applications of the A24 data set of accurate interaction energies, *Phys. Chem. Chem. Phys.* **17**, 19268 (2015).
 - [39] T. Tsatsoulis, F. Hummel, D. Usvyat, M. Schütz, G. H. Booth, S. S. Binnie, M. J. Gillan, D. Alfè, A. Michaelides, and A. Grüneis, A comparison between quantum chemistry and quantum monte carlo techniques for the adsorption of water on the (001) lih surface, *J. Chem. Phys.* **146**, 204108 (2017).
 - [40] S. Grimme, Supramolecular binding thermodynamics by dispersion-corrected density functional theory, *Chemistry - A European Journal* **18**, 9955 (2012).
 - [41] R. Sure and S. Grimme, Comprehensive Benchmark of Association (Free) Energies of Realistic Host-Guest Complexes, *Journal of Chemical Theory and Computation* **11**, 3785 (2015).
 - [42] J. Hermann, D. Alfè, and A. Tkatchenko, Nanoscale π - π Stacked molecules are bound by collective charge fluctuations, *Nat. Commun.* **8**, 14052 (2017).
 - [43] J. Calbo, E. Ortí, J. C. Sancho-García, and J. Aragó, Accurate treatment of large supramolecular complexes by double-hybrid density functionals coupled with nonlocal van der waals corrections, *J. Chem. Theor. Comput.* **11**, 932 (2015).
 - [44] J. Calbo, E. Ortí, J. C. Sancho-García, and J. Aragó, Accurate treatment of large supramolecular complexes by double-hybrid density functionals coupled with nonlocal van der waals corrections, *J. Chem. Theory Comput.* **11**, 932 (2015).
 - [45] A. S. Christensen, M. Elstner, and Q. Cui, Improving intermolecular interactions in DFTB3 using extended polarization from chemical-potential equalization, *J. Chem. Phys.* **143**, 084123 (2015).
 - [46] J. G. Brandenburg, C. Bannwarth, A. Hansen, and S. Grimme, B97-3c: A revised low-cost variant of the B97-D density functional method, *J. Chem. Phys.* **148**, 064104 (2018).
 - [47] K. Carter-Fenk, K. U. Lao, K.-Y. Liu, and J. M. Herbert, Accurate and efficient ab initio calculations for supramolecular complexes: Symmetry-adapted perturbation theory with many-body dispersion, *J. Phys. Chem. Lett.* **10**, 2706 (2019).
 - [48] R. A. Kendall, T. H. Dunning Jr., and R. J. Harrison, Electron affinities of the first-row atoms revisited. Systematic basis sets and wave functions, *J. Chem. Phys.* **96**, 6796 (1992).
 - [49] T. Helgaker, W. Klopper, H. Koch, and J. Noga, Basis-set convergence of correlated calculations on water, *J. Chem. Phys.* **106**, 9639 (1997).

- [50] S. F. Boys and F. Bernardi, The calculation of small molecular interactions by the differences of separate total energies. Some procedures with reduced errors, *Mol. Phys.* **19**, 553 (1970).
- [51] The error is estimated as the difference of the two best converged results, i.e., the deviation of interaction energies using Tight and very Tight LNO settings and CBS(Q,5) with and without CP correction. The compound error of the two sources is obtained as the sum of the absolute error estimates, thus the potential cancellation of errors is not taken into account.
- [52] M. Kállay, P. R. Nagy, D. Mester, Z. Rolik, G. Samu, J. Csontos, J. Csóka, P. B. Szabó, L. Gyevi-Nagy, B. Hégyel, I. Ladjánszki, L. Szegedy, B. Ladóczki, K. Petrov, M. Farkas, P. D. Mezei, and Á. Ganyecz, The MRCC program system: Accurate quantum chemistry from water to proteins, *J. Chem. Phys.* **152**, 074107 (2020).
- [53] A. Zen, S. Sorella, M. J. Gillan, A. Michaelides, and D. Alfè, Boosting the accuracy and speed of quantum Monte Carlo: Size consistency and time step, *Phys. Rev. B* **93**, 241118 (2016).
- [54] A. Zen, J. G. Brandenburg, A. Michaelides, and D. Alfè, A new scheme for fixed node diffusion quantum Monte Carlo with pseudopotentials: Improving reproducibility and reducing the trial-wave-function bias, *J. Chem. Phys.* **151**, 134105 (2019).
- [55] M. A. Morales, J. McMinis, B. K. Clark, J. Kim, and G. E. Scuseria, Multideterminant Wave Functions in Quantum Monte Carlo, *J. Chem. Theor. Comput.* **8**, 2181 (2012).
- [56] A. Scemama, T. Applencourt, E. Giner, and M. Caffarel, Quantum Monte Carlo with very large multideterminant wavefunctions, *J. Comp. Chem.* **37**, 1866 (2016).
- [57] C. Genovese, A. Meninno, and S. Sorella, Assessing the accuracy of the Jastrow antisymmetrized geminal power in the H 4 model system, *J. Chem. Phys.* **150**, 084102 (2019).
- [58] J. R. Trail and R. J. Needs, Smooth relativistic Hartree-Fock pseudopotentials for H to Ba and Lu to Hg, *J. Chem. Phys.* **122**, 174109 (2005).
- [59] J. R. Trail and R. J. Needs, Norm-conserving Hartree-Fock pseudopotentials and their asymptotic behavior, *J. Chem. Phys.* **122**, 014112 (2005).
- [60] J. R. Trail and R. J. Needs, Pseudopotentials for correlated electron systems, *J. Chem. Phys.* **139**, 014101 (2013).
- [61] D. Pfau, J. S. Spencer, A. G. de G. Matthews, and W. M. C. Foulkes, Ab-initio solution of the many-electron Schrödinger equation with deep neural networks, arXiv e-prints, arXiv:1909.02487 (2019).
- [62] J. Hermann, Z. Schätzle, and F. Noé, Deep neural network solution of the electronic

- Schrödinger equation, arXiv e-prints , arXiv:1909.08423 (2019).
- [63] M. Gordon, ed., *Fragmentation: Toward Accurate Calculations on Complex Molecular Systems* (Wiley, New York, 2017).
- [64] J. F. Gonthier and M. Head-Gordon, Assessing electronic structure methods for long-range three-body dispersion interactions: Analysis and calculations on well-separated metal atom trimers, *J. Chem. Theory Comput.* **15**, 4351 (2019).
- [65] M. Kállay and J. Gauss, Approximate treatment of higher excitations in coupled-cluster theory, *J. Chem. Phys.* **123**, 214105 (2005).
- [66] J. A. Frey, C. Holzer, W. Klopper, and S. Leutwyler, Experimental and theoretical determination of dissociation energies of dispersion-dominated aromatic molecular complexes, *Chem. Rev.* **116**, 5614 (2016).
- [67] T. Kawase, K. Tanaka, N. Fujiwara, H. R. Darabi, and M. Oda, Complexation of a Carbon Nanoring with Fullerenes, *Angew. Chem. Int. Ed.* **42**, 1624 (2003).
- [68] J. ezáč, P. Jurečka, K. E. Riley, J. Černý, H. Valdes, K. Pluháčková, K. Berka, T. Řezáč, M. Pitoňák, J. Vondrášek, and P. Hobza, Quantum Chemical Benchmark Energy and Geometry Database for Molecular Clusters and Complex Molecular Systems (www.begdb.com): A Users Manual and Examples, *Collect. Czech. Chem. Commun.* **73**, 1261 (2008).
- [69] T. Iwamoto, Y. Watanabe, T. Sadahiro, T. Haino, and S. Yamago, Size-selective encapsulation of c60 by [10]cycloparaphenylene: Formation of the shortest fullerene-peapod, *Angew. Chem. Int. Ed* **50**, 8342 (2011).
- [70] J. Antony, R. Sure, and S. Grimme, Using dispersion-corrected density functional theory to understand supramolecular binding thermodynamics, *Chem. Commun.* **51**, 1764 (2015).
- [71] P. R. Nagy and M. Kállay, Optimization of the linear-scaling local natural orbital CCSD(T) method: Redundancy-free triples correction using Laplace transform, *J. Chem. Phys.* **146**, 214106 (2017).
- [72] L. Gyevi-Nagy, M. Kállay, and P. R. Nagy, Integral-direct and parallel implementation of the CCSD(T) method: Algorithmic developments and large-scale applications, *J. Chem. Theory Comput.* **16**, 336 (2020).
- [73] R. J. Needs, M. D. Towler, N. D. Drummond, and P. López Ríos, Continuum variational and diffusion quantum Monte Carlo calculations, *J. Phys. Condens. Matter* **22**, 023201 (2010).
- [74] L. Mitáš, E. L. Shirley, and D. M. Ceperley, Nonlocal pseudopotentials and diffusion Monte

- Carlo, *J. Chem. Phys.* **95**, 3467 (1991).
- [75] M. Casula, Beyond the locality approximation in the standard diffusion Monte Carlo method, *Phys. Rev. B* **74**, 161102 (2006).
- [76] P. Giannozzi, S. Baroni, N. Bonini, M. Calandra, R. Car, C. Cavazzoni, D. Ceresoli, G. L. Chiarotti, M. Cococcioni, I. Dabo, *et al.*, QUANTUM ESPRESSO: a modular and open-source software project for quantum simulations of materials, *J. Phys. Condens. Matter* **21**, 395502 (2009).
- [77] Z. Rolik, L. Szegedy, I. Ladjánszki, B. Ladóczki, and M. Kállay, An efficient linear-scaling CCSD(T) method based on local natural orbitals, *J. Chem. Phys.* **139**, 094105 (2013).
- [78] P. R. Nagy, G. Samu, and M. Kállay, An integral-direct linear-scaling second-order Møller–Plesset approach, *J. Chem. Theory Comput.* **12**, 4897 (2016).
- [79] Z. Rolik and M. Kállay, A general-order local coupled-cluster method based on the cluster-in-molecule approach, *J. Chem. Phys.* **135**, 104111 (2011).
- [80] M. Kállay, Linear-scaling implementation of the direct random-phase approximation, *J. Chem. Phys.* **142**, 204105 (2015).
- [81] A. Karton and J. M. L. Martin, Comment on: “Estimating the Hartree–Fock limit from finite basis set calculations”, *Theor. Chem. Acc.* **115**, 330 (2006).
- [82] B. P. Prascher, D. E. Woon, K. A. Peterson, T. H. Dunning, and A. K. Wilson, Gaussian basis sets for use in correlated molecular calculations. VII. Valence, core-valence, and scalar relativistic basis sets for Li, Be, Na, and Mg, *Theor. Chem. Acc.* **128**, 69 (2011).
- [83] T. J. Lee and P. R. Taylor, A diagnostic for determining the quality of single-reference electron correlation methods, *Int. J. Quantum Chem.* **36**, 199 (1989).
- [84] N. Sylvetsky, A. Banerjee, M. Alonso, and J. M. L. Martin, Performance of localized coupled cluster methods in a moderately strong correlation regime: Hückel–Möbius interconversions in expanded porphyrins, *J. Chem. Theory Comput.* **16**, 3641 (2020).
- [85] J. Řezáč, K. E. Riley, and P. Hobza, S66: A well-balanced database of benchmark interaction energies relevant to biomolecular structures, *J. Chem. Theory Comput.* **7**, 2427 (2011).